Supporting Information

Nanoparticle Surface Engineering with Heparosan Polysaccharide Reduces Serum Protein Adsorption and Enhances Cellular Uptake

Wen Yang[1], Lin Wang[1], Mulin Fang[2], Vinit Sheth[1], Yushan Zhang[3], Alyssa M. Holden[1], Nathan D. Donahue[1], Dixy E. Green[4], Alex N. Frickenstein[1], Evan M. Mettenbrink[1], Tyler A. Schwemley[1], Emmy R. Francek[1], Majood Haddad[1], Md Nazir Hossen[5], Shirsha Mukherjee[1], Si Wu[2], Paul L. DeAngelis[4], and Stefan Wilhelm[1,6,7*]

[1] Stephenson School of Biomedical Engineering, University of Oklahoma, Norman, Oklahoma, 73019, USA

[2] Department of Chemistry and Biochemistry, University of Oklahoma, Norman, OK, 73019, USA

[3] Department of Pathology, University of Oklahoma Health Sciences Center, Oklahoma City, Oklahoma 73104, USA

[4] Department of Biochemistry and Molecular Biology, University of Oklahoma Health Sciences Center, Oklahoma City, Oklahoma, 73104, USA

[5] Department of Pharmaceutical and Biomedical Sciences, College of Pharmacy, California Northstate University, Elk Grove, CA, 95757, USA

[6] Stephenson Cancer Center, University of Oklahoma Health Sciences Center, Oklahoma City, Oklahoma, 73104, USA

[7] Institute for Biomedical Engineering, Science, and Technology (IBEST), University of Oklahoma, Norman, Oklahoma, 73019, USA

[*] Corresponding author: Stefan Wilhelm, Ph.D.

Email Addresses: stefan.wilhelm@ou.edu

ORCID: Stefan Wilhelm 0000-0003-2167-6221

Table of Contents

Figures

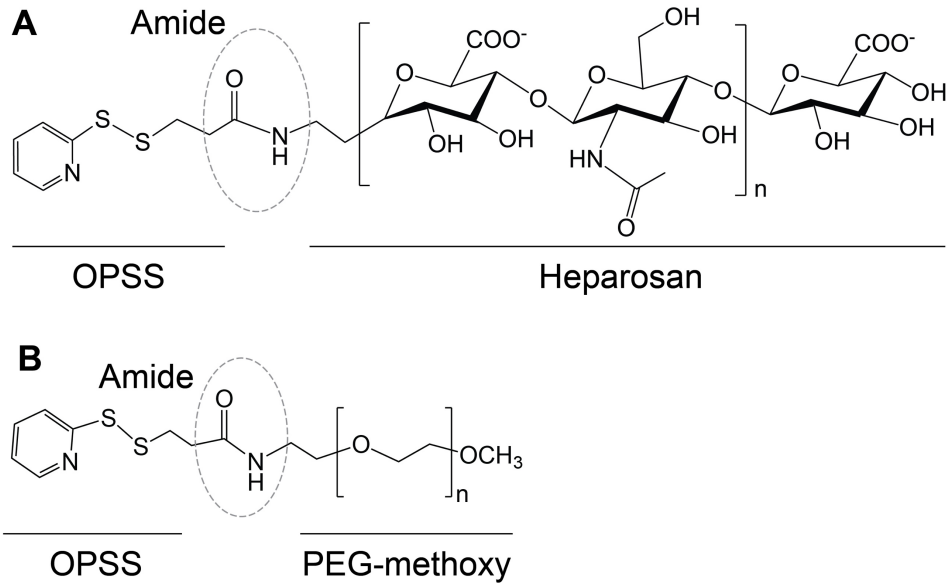

Figure S1. Chemical structure of OPSS-HEP, and OPSS-PEG.

Chemical structures of OPSS-conjugated heparosan **(A)** or OPSS-conjugated PEG **(B)**.

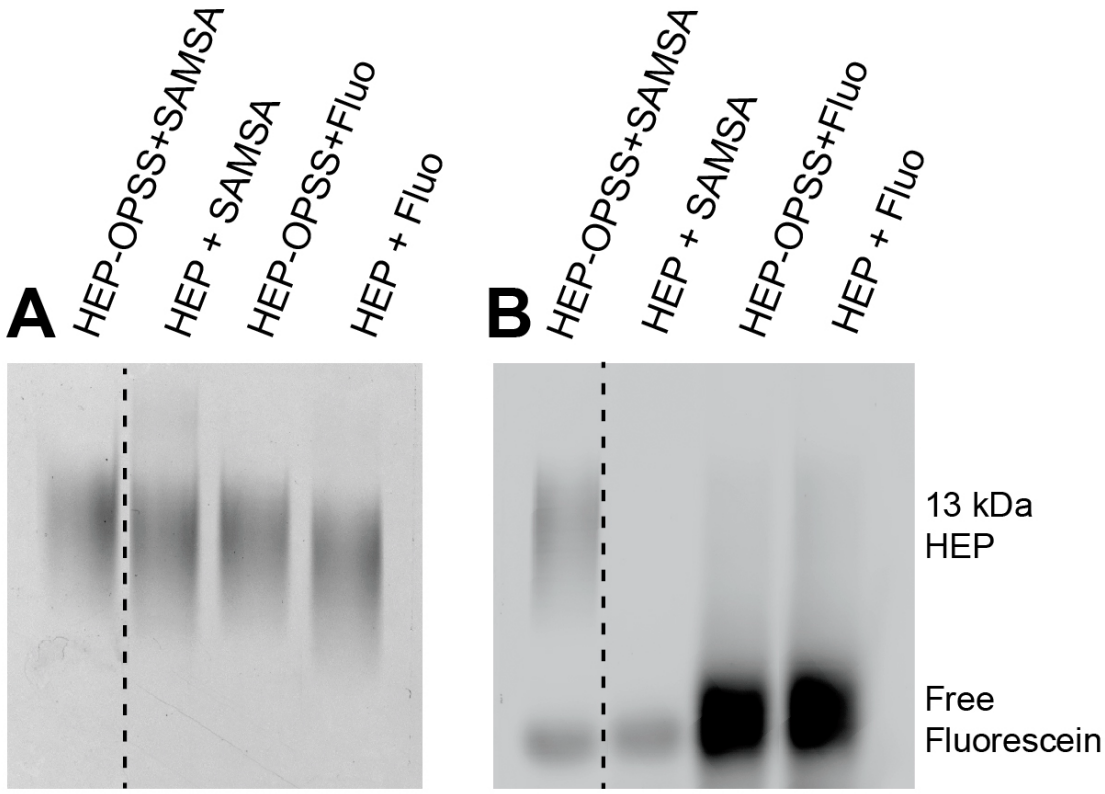

Figure S2. Characterization of the OPSS-HEP conjugation.

(A) Characterization of heparosan and its OPSS-derivative by PAGE gel. Alcian Blue-staining of the gel shows the presence of heparosan polysaccharide **(B)** Analysis of OPSS-HEP chemical reactivity via fluorescent probes: Activated SAMSA (a fluorescent group with a free thiol after deprotection) reactivity and fluorescein-5-maleimide (Fluo; a fluorescent sulfhydryl reactive reagent) reactivity were employed to qualitatively evaluate OPSS conjugation and degradation (i.e., any loss of the OPS group reveals a free thiol), respectively. The fluorescent SAMSA reaction product with OPSS-HEP aligned well with the polysaccharide bands in the Alcian blue gel, indicating that the conjugation of OPSS with HEP was effective. No fluorescent product was observed in the fluorescein-5-maleimide reactions indicating the absence of free thiol groups; therefore, no significant degradation of the OPSS-HEP was detected during handling and storage. Images are cropped and gel lanes fused as indicated with the dashed lines. Original images are available upon request.

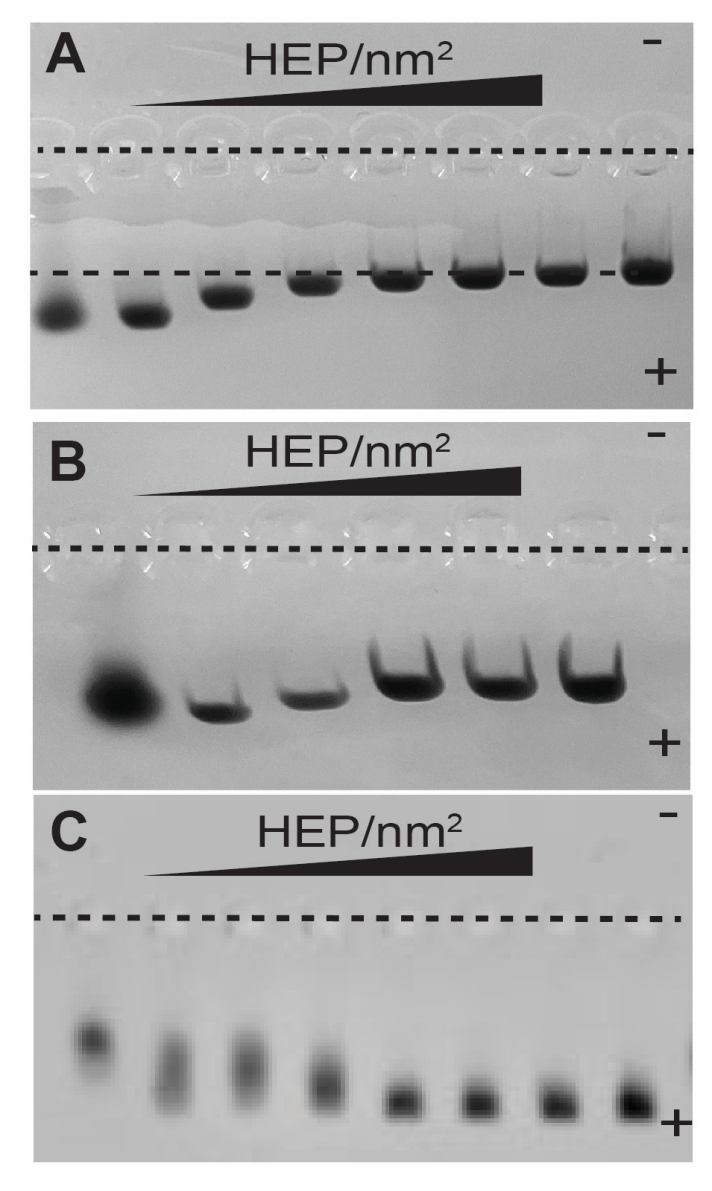

Figure S3. Agarose gel electrophoresis images of 15-nm HEP-AuNPs.

(A), (C) Agarose gel electrophoresis of heparosan-modified AuNPs by salt aging (A) or by simple mixing (C). The coating reactions contained various ratios of HEP to AuNPs ranging from 0, 0.1, 0.25, 0.5, 0.75, 1, 1.5, or 2 HEP/nm^2. The addition of HEP chains to the AuNPs slows migration, possibly due to the increase in hydrodynamic size until a plateau indicates surface saturation. **(B)** Agarose gel electrophoresis of heparosan-modified AuNPs by pH method. The surface HEP densities were 0, 0.25, 0.5, 1, 2, or 5 HEP/nm^2. The *dashed lines* indicate the position of the wells.

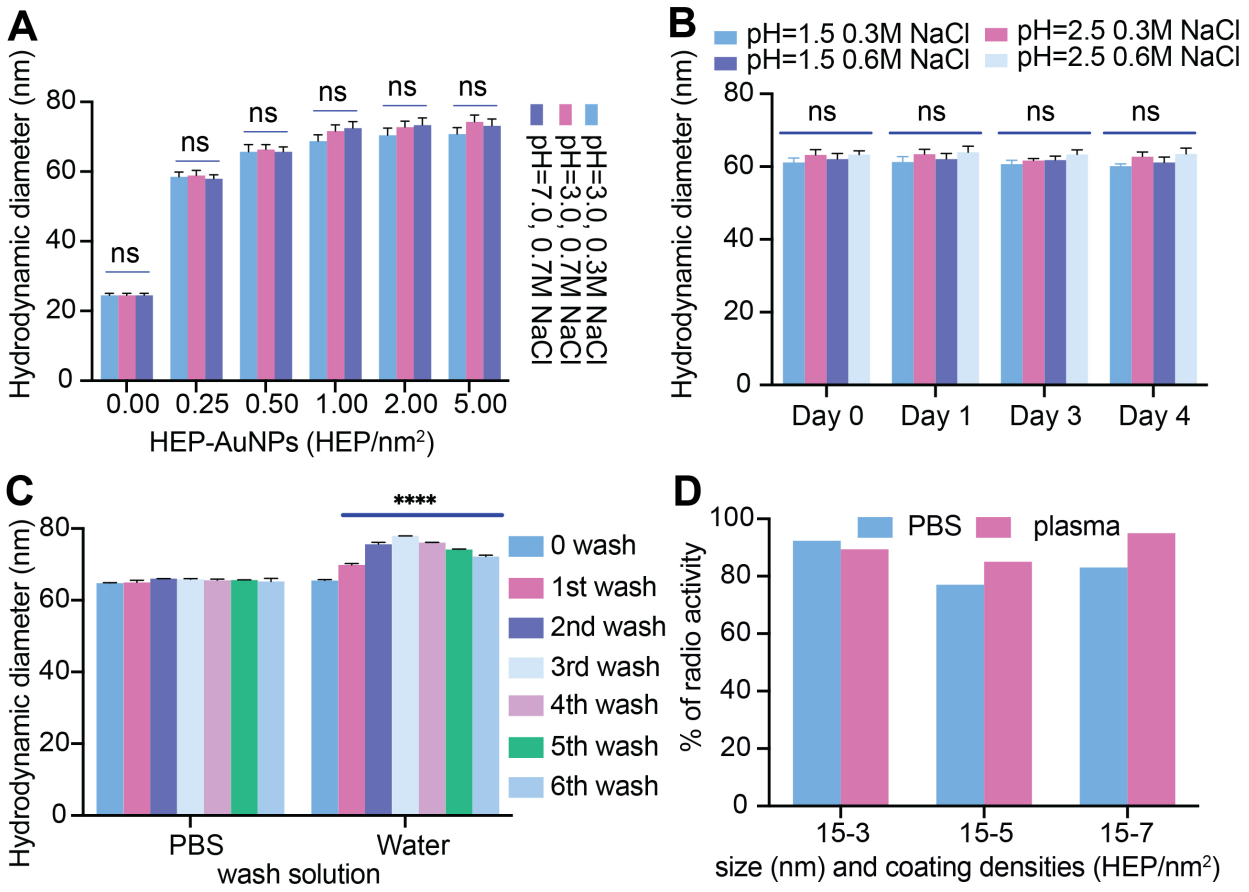

Figure S4. Nanoparticle colloidal stability of 15-nm HEP-AuNPs.

(A-B) Nanoparticle colloidal stability in buffers with different sodium chloride (NaCl) concentrations and pH (A) and over 4 days (B). **(C)** Nanoparticle colloidal stability after repeated centrifugation and washing by water and PBS. Bar graphs indicate mean ± s.d. of biological triplicates. Statistical tests were performed by Two-Way ANOVA ($p<0.0001$ (****); n.s. indicates no statistically significant differences. **(D)** Plasma challenging of radiolabeled HEP-AuNPs with different coating reaction ratios and sizes. For example, 15-3 indicates 15-nm AuNPs with calculated addition ratios of 3 HEP per nm^2 of particle surface area in the coating reaction. The incubation time for 15-3 was 12h, 15-5 was 24 hours, and 15-7 was 48 hours.

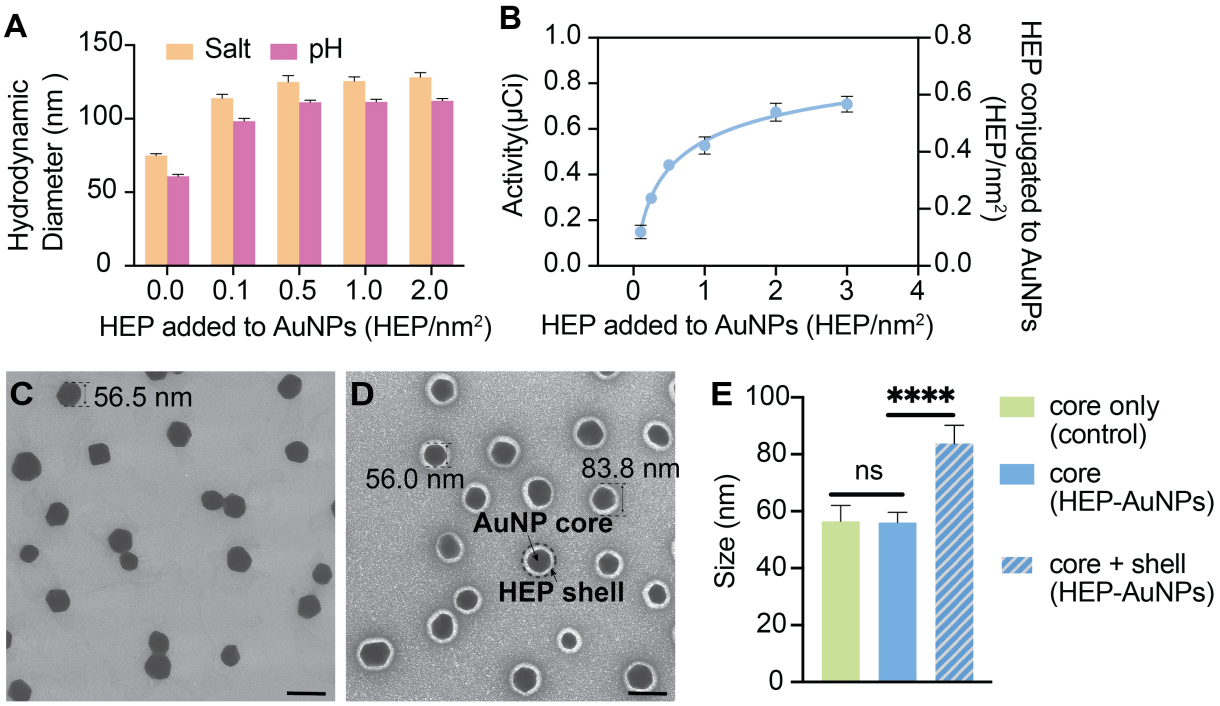

Figure S5. Physicochemical characterization of 55-nm HEP-AuNPs.

(A) Dynamic light scattering (DLS) was used to measure the hydrodynamic diameter of 55-nm AuNPs after mixing with various amounts of HEP per nm^2 of nanoparticle surface area by either the salt concentration (salt aging) or pH methods. Bars indicate mean ± SD (n=3). **(B)** Radiochemical assay of HEP incorporation onto AuNPs: Various amounts of radiolabeled heparosan were mixed with 55-nm AuNPs, and after the coating process, free HEP was washed away. The left y-axis reports the [^{3}H] radioactivity of different HEP coating levels. The right y-axis represents the actual HEP per nm^2 calculated from the specific radioactivity of [^{3}H]HEP-OPSS. **(C), (D)** Representative TEM micrograph of 55-nm citrate coated AuNPs with a diameter of 56.5 ± 5.6nm (C) and HEP-AuNPs The light grey halo or shell around the dark AuNP core (56.0 ± 3.5 nm) corresponds to surface conjugated HEP (panel D; 83.8 ± 6.5 nm) denoted here as the 'HEP shell'. **(E)** TEM micrograph image analysis of nanoparticle size. The *x*-axis labels are as follows: Core only (citrate coated AuNPs as control from panel C; green bar); Core of HEP-AuNPs from panel D (Core diameter of HEP-AuNPs in panel D; blue bar); Core + shell of HEP-AuNPs (Core and shell diameter of HEP-AuNPs from panel D; slanted lined blue bar). Bars indicate mean ± SD. Statistical tests were performed by one-way ANOVA ($p<0.0001$ (****); n.s. indicates no statistically significant differences). Scale bars denote 100 nm.

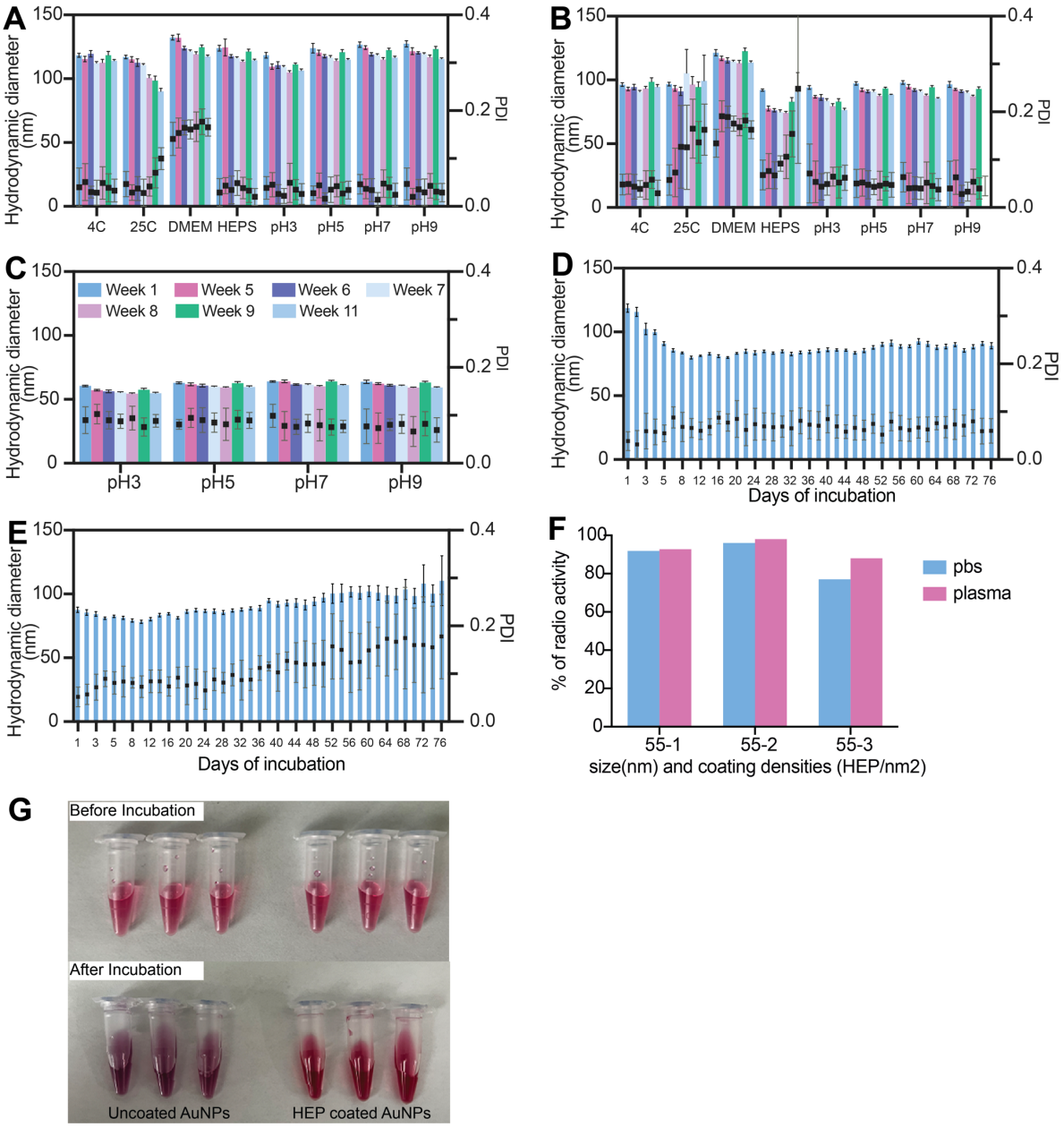

Figure S6. Nanoparticle colloidal stability of 55-nm HEP-AuNPs.

(A-C) Long-term colloidal stability of 55-nm HEP-AuNPs (A), PEG-AuNPs (B), or Citrate-AuNPs (C) under different conditions over 11 weeks. Panels A and B share the same legend as shown in Panel C. **(D- (E)** Colloidal stability of 55-nm HEP-AuNPs (D) and PEG-AuNPs (E) after FBS incubation at 37ºC for 76 days. Bars indicate mean ± SD. Dots represent the polydispersity index (PDI). **(F)** Plasma challenging of radiolabeled HEP-AuNPs with different coating densities, e.g., 5-1 indicates 55-nm AuNPs with the addition of 1 HEP per nm^2. The incubation time was 24 h. **(G)** Photographs of uncoated AuNPs (left) or HEP-coated AuNPs (right) before and after incubation in cell media without FBS. The red color indicates colloidal stability, while the blue color indicates nanoparticle aggregation.

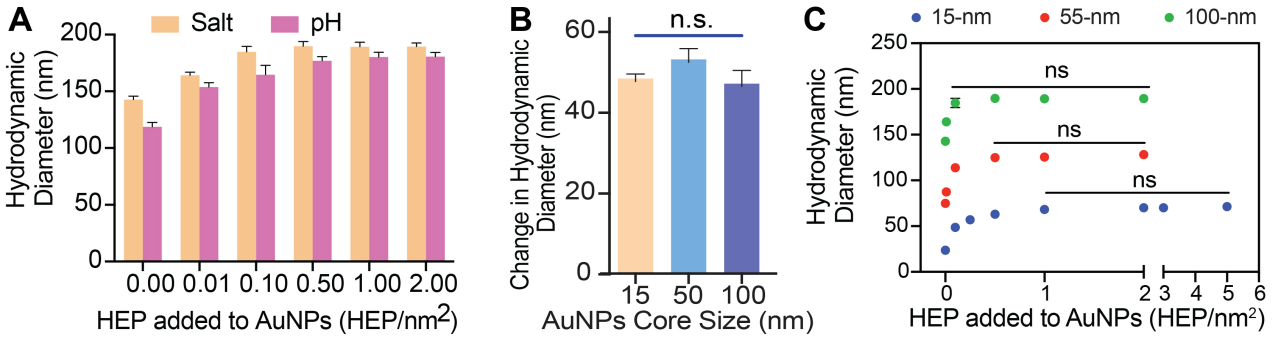

Figure S7. Characterization of 100-nm HEP-AuNPs and summary of HEP-AuNPs.

(A) Dynamic light scattering (DLS) was used to measure the hydrodynamic diameter of 100-nm AuNPs after mixing with various amounts of HEP per nm^2 of nanoparticle surface area by salt concentration (salt aging) or pH methods. Bars indicate mean ± SD (n=3). **(B)** The hydrodynamic diameter changes from 0 HEP/nm^2 to HEP saturated point (2 HEP/nm^2) calculated from dynamic light scattering data. Bars indicate mean ± SD. Statistical tests were performed by one-way ANOVA (n.s. indicates no statistically significant differences). **(C)** The saturation curves of heparosan on 15-nm, 55-nm, and 100-nm nanoparticles were measured by dynamic light scattering. Possibly due to a reduction in overall nanoparticle curvature with increasing nanoparticle size, the maximum achievable HEP surface coating densities of 15-nm, 55-nm, and 100-nm AuNPs were ~1.0 HEP/nm^2, ~0.5 HEP/nm^2, and ~0.1 HEP/nm^2, respectively. Statistical tests were performed by one-way ANOVA (n.s. indicates no statistically significant differences)

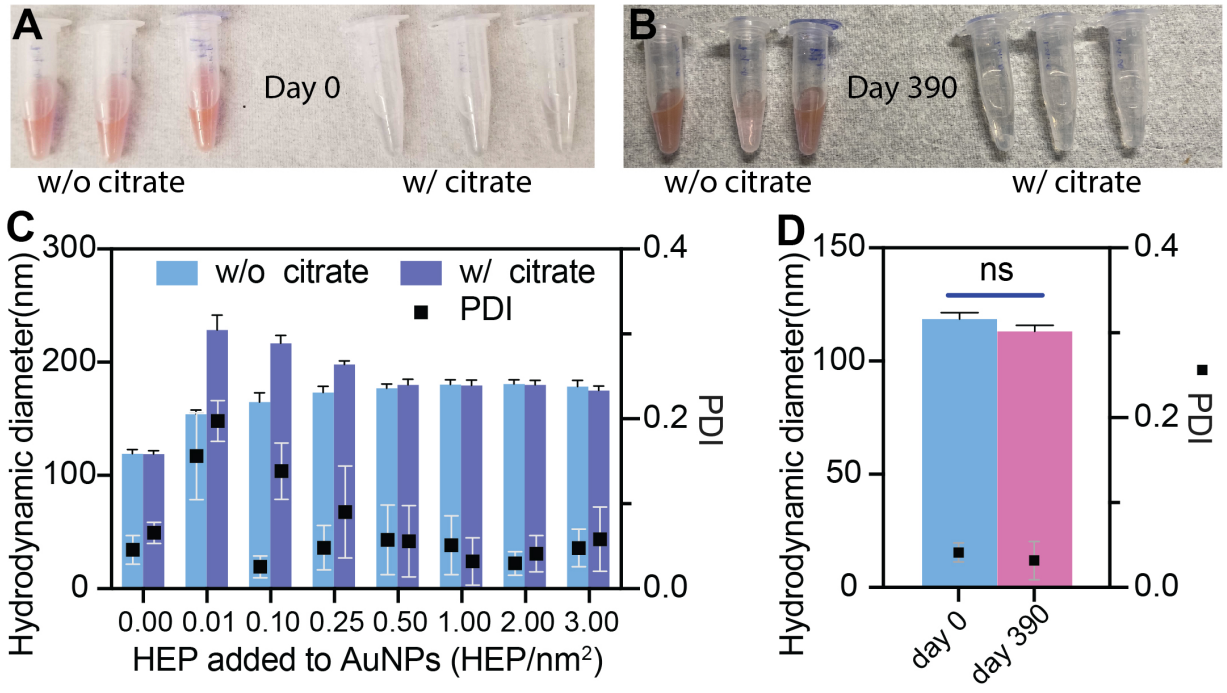

Figure S8. Optimized pH method for maintaining colloidal stability of 100-nm AuNPs modified with low HEP densities.

(A-B) Photographs of 100-nm AuNPs coated with 0.01 HEP per nm^2 using the pH method with citrate and without citrate after 0 days (A) and 390 days (B). The clear solutions indicate nanoparticle aggregation when citrate is present. **(C)** Dynamic light scattering (DLS) was used to measure the hydrodynamic diameter of 100-nm AuNPs after mixing with various amounts of HEP per nm^2 of nanoparticle surface area by pH method with citrate and without citrate. **(D)** The hydrodynamic diameter changes of HEP-AuNP with 0.01 HEP per nm^2 by pH method without citrate after 390 days. Bars indicate mean ± SD. Dots represent PDI. Statistical test was performed by unpaired T-test (n.s. indicates no statistically significant differences)

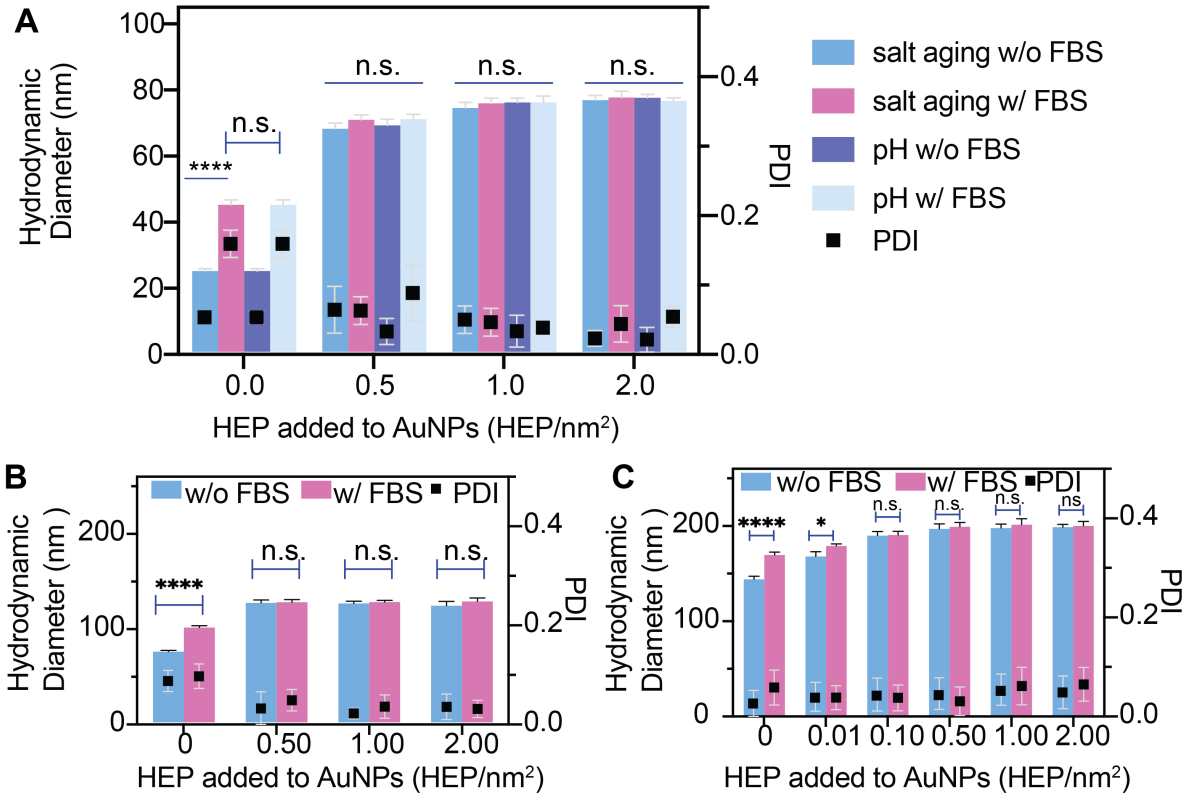

Figure S9. FBS incubation of 15-nm, 55-nm, or 100-nm HEP-AuNPs by salt aging.

(A-C) Dynamic light scattering (DLS) was used to measure the effect of FBS incubation with controls (without FBS) of AuNPs mixed with different surface HEP densities with AuNPs sizes of 15-nm (A), 55-nm (B), or 100-nm (C). The increased polydispersity index (PDI) indicates a broader nanoparticle size distribution during FBS incubation. Bar graphs indicate mean ± SD (n=3). Statistical tests were performed by one-way ANOVA ($p<0.0001$ (****); $p<0.05$(*); n.s. indicates no statistically significant differences).

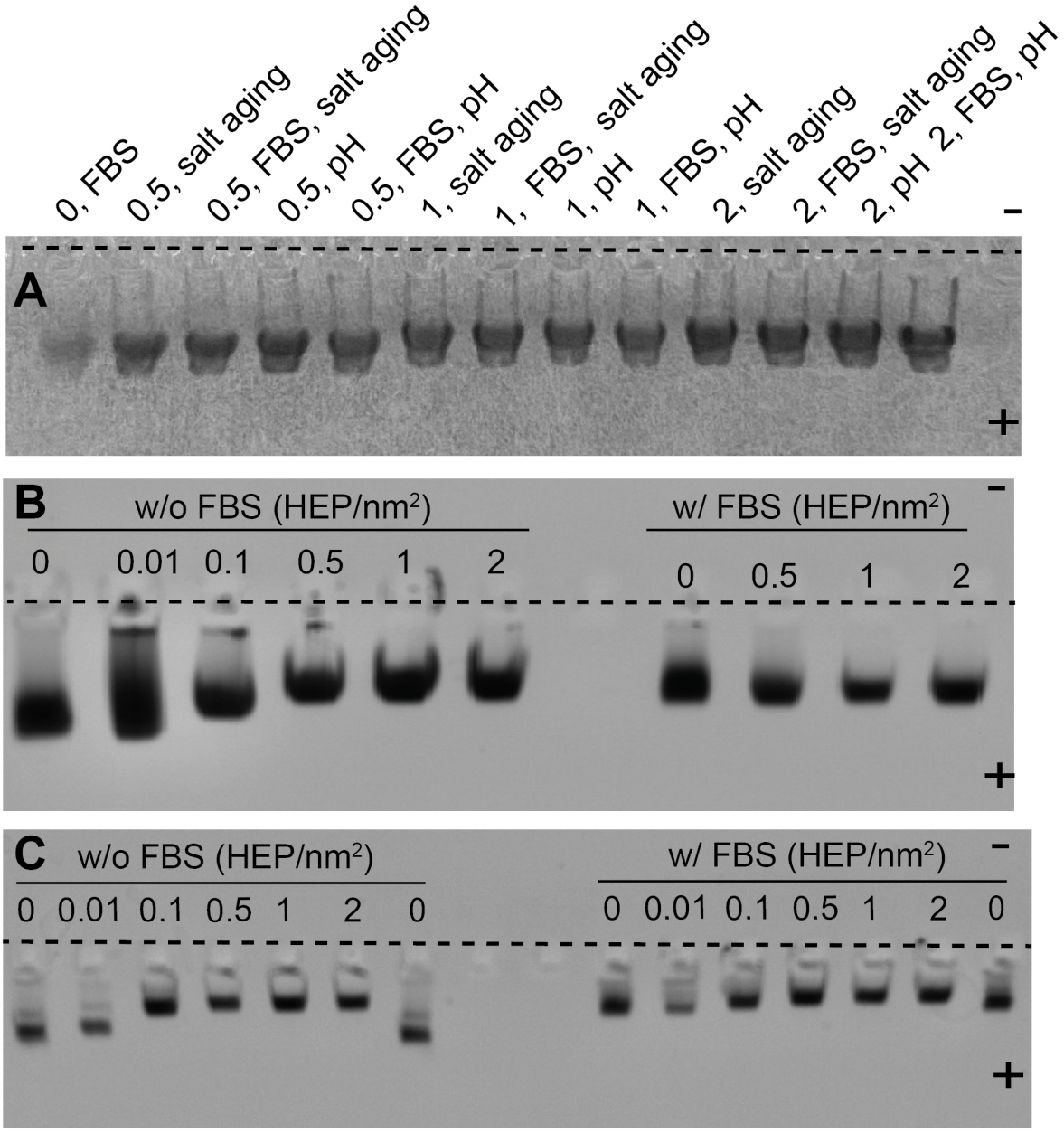

Figure S10. Agarose gel electrophoresis images of HEP-AuNPs upon FBS incubation.

(A-C) AuNPs of different sizes were compared: 15-nm (A), 55-nm (B), 100-nm (C). *Dashed lines* indicate the position of the wells.

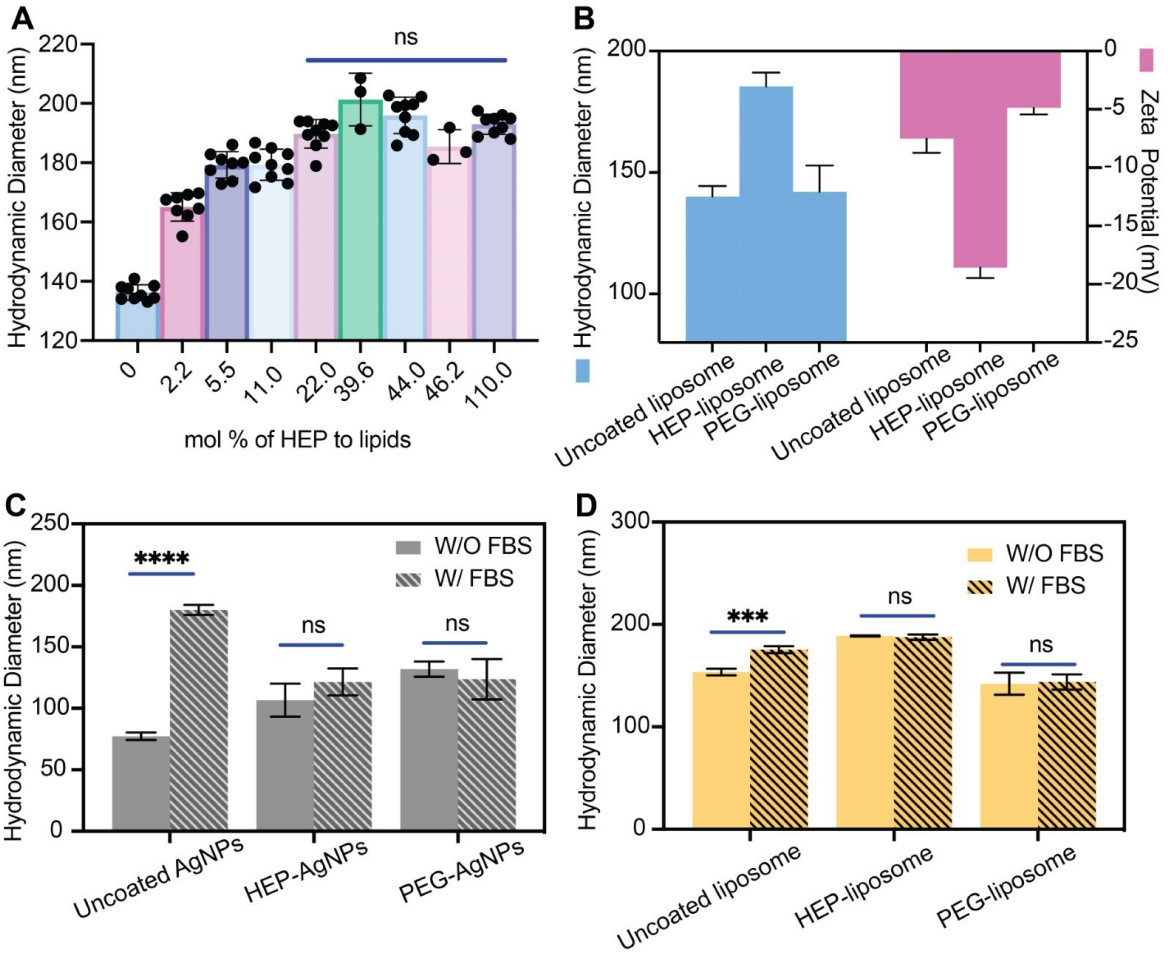

Figure S11. Heparosan coating reduces protein corona formation on silver nanoparticles and liposomes.

(A) Dynamic light scattering (DLS) was used to measure the hydrodynamic diameter of heparosan-coated liposomes with various mole percentages of HEP-dipalmitate lipid (added by post-insertional modification of pre-formed liposomes). **(B)** Hydrodynamic size and zeta potential of the uncoated liposome, HEP-liposome, or PEG-liposome preparations were measured by DLS. **(C-D)** DLS was used to compare the hydrodynamic diameter differences before and after FBS incubation (*slanted lined bars* stand for incubation with FBS) of silver nanoparticles (panel C; gray) or liposome nanoparticles (panel D; yellow). Bars indicate mean ± SD.

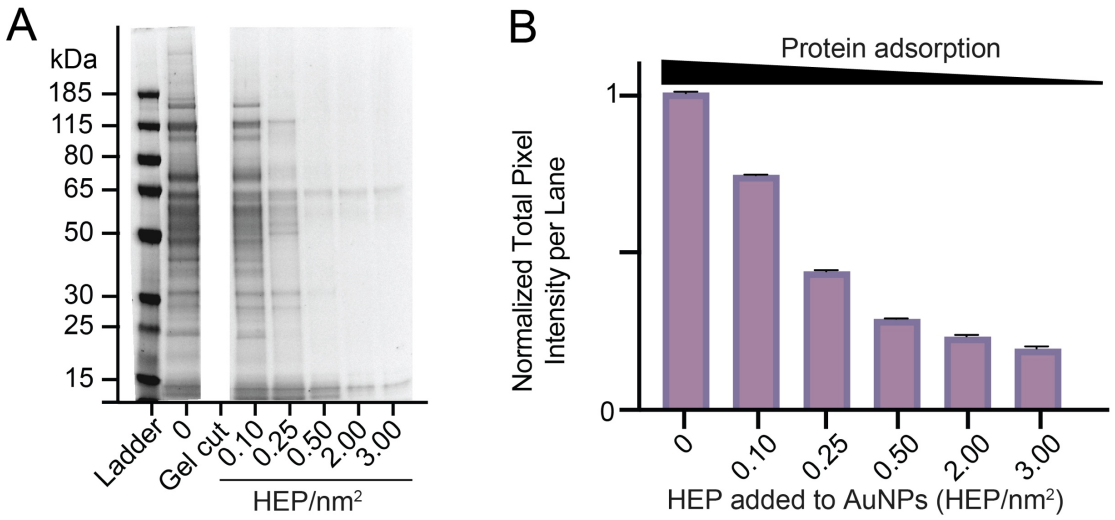

Figure S12. Heparosan coating reduces protein corona formation on 15-nm AuNPs.

(A) The qualitative molecular composition of the adsorbed FBS proteins layer on 15-nm AuNPs with various amounts of HEP in the coating reactions by SDS-PAGE gel. The lanes on the right side and left side of this image are from the same gel. **(B)** SDS-PAGE image analysis of each lane. Data points are normalized to the start point (0 HEP/nm^2). Bars indicate mean ± SD.

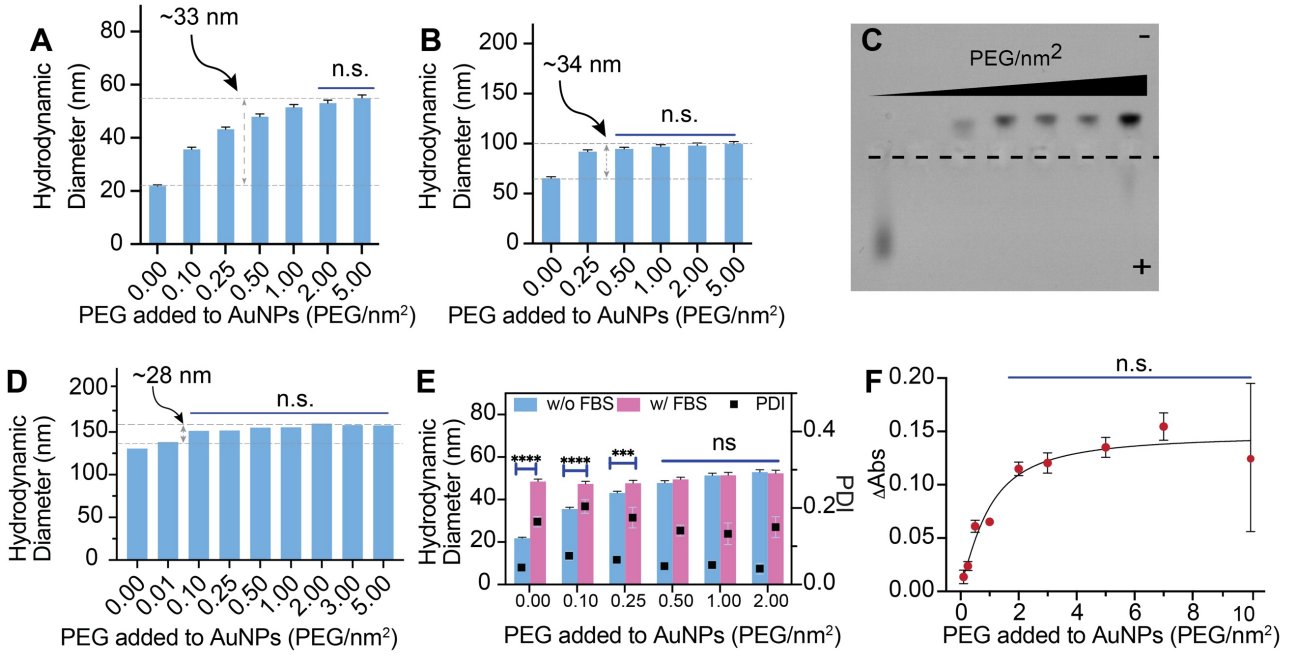

Figure S13. Physicochemical characterization of PEG-AuNPs.

(A), (B) and (D) Dynamic light scattering (DLS) was used to measure the hydrodynamic diameter of PEGylated 15-nm(A), 55-nm(B), or 100-nm AuNPs (D). Bars indicate mean ± SD (n=3). **(C)** Agarose gel electrophoresis of PEG-modified AuNPs incubation with FBS. Dashed lines indicate the position of the wells. **(E)** Dynamic light scattering (DLS) was used to measure the FBS incubation with control (without FBS) of AuNPs mixed with different surface PEG densities with AuNPs size of 15-nm. The increased polydispersity index (PDI) indicates a broader size distribution caused by FBS incubation. Bar graphs indicate mean ± SD (n=3). **(F)** An UV-Vis spectrophotometry-based depletion assay to quantify the maximum loading capacity of PEG. Statistical tests were performed by one-way ANOVA ($p<0.0001$ (****); $p<0.05$(*); n.s. indicates no statistically significant differences.

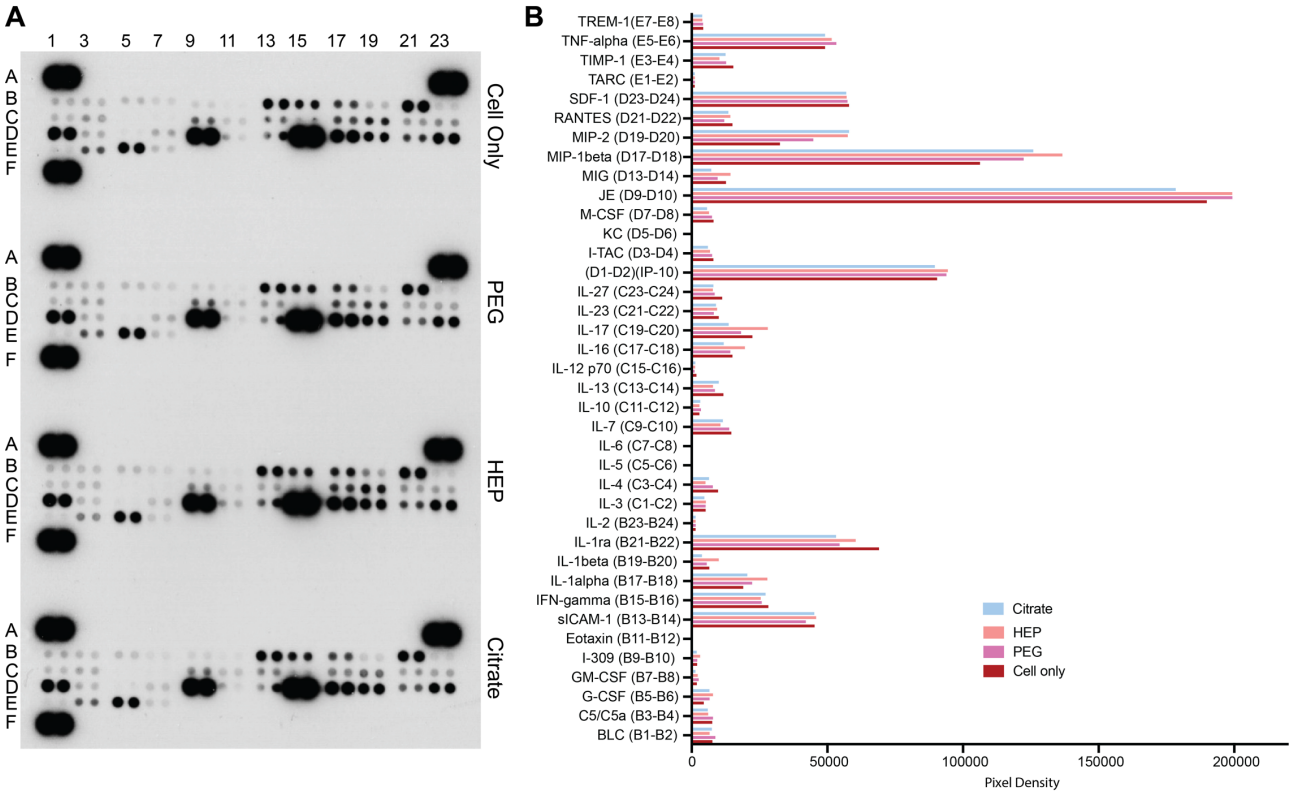

Figure S14. Assessment of cytokine release levels.

(A-B) Cytokine release levels in the supernatant of RAW 264.7 macrophages after 24 h incubation with citrate AuNPs, PEG-AuNPs, or HEP-AuNPs were determined using an array of specific antibodies (A). The signal intensities in panel A were quantified using the Quick Spot image analysis tool (B). Data points of D11-12 and D15-16 were excluded for analysis due to the interference of the nearby strong signal. A1-2, A23-24, F1-2 are reference spots; F23-24 are negative control spots.

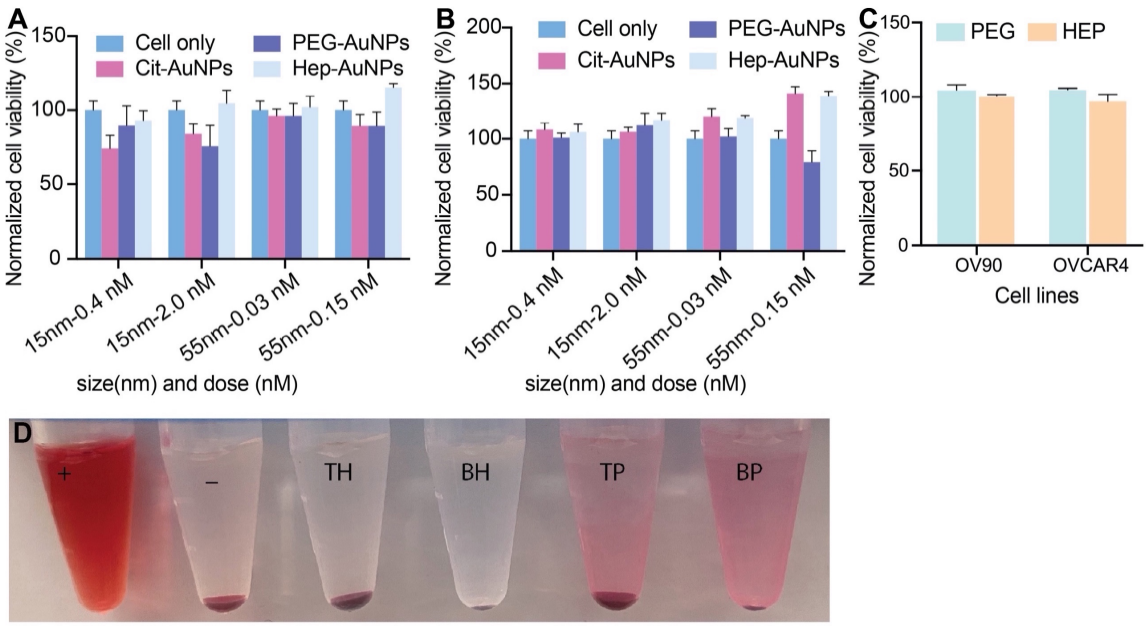

Figure S15. Cytotoxicity and hemolysis tests using HEP- or PEG-AuNPs.

(A-B) Cell viability of RAW 264.7 macrophages treated with different sizes and doses of HEP-AuNPs or PEG- AuNPs for 24 (A) and 48 (B) hours by XTT. Bar graphs indicate mean ± SD (n=5). **(C)** Cell viability test on OV90 cells and OVCAR4 cells treated with 0.1-nM HEP-AuNPs or PEG-AuNPs by XTT assay. Bar graphs indicate mean ± SD (n=5). **(D)** Photographs of AuNPs incubated with human red blood cells. From left to right: +, positive control; -, PBS negative control; TH, HEP-AuNPs with blood cells; BH, HEP-AuNPs without blood cells; TP, PEG-AuNPs with blood cells; BP, PEG-AuNPs without blood cells.

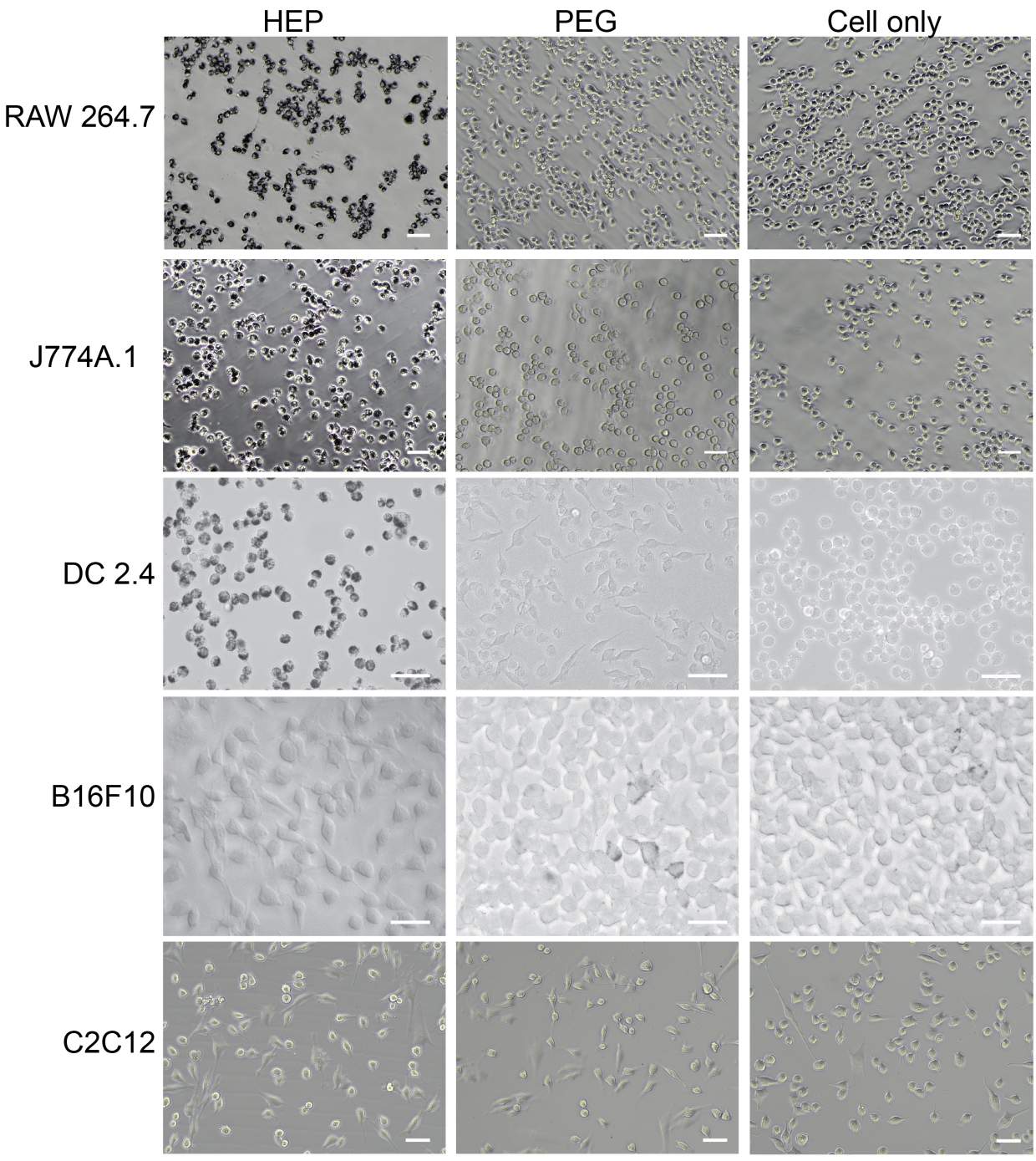

Figure S16. Light micrographs of different cell types after incubation with 55-nm HEP-AuNPs.

Either 0.2nM HEP-AuNPs or PEG-AuNPs were incubated with RAW 264.7, J774A.1 macrophages, DC2.4 dendritic cells, B16F10 melanoma, or C2C12 muscle cells for 6 hours. Cells were imaged with a brightfield light microscope after removing uninternalized AuNPs. Scale bars represent 50 μm.

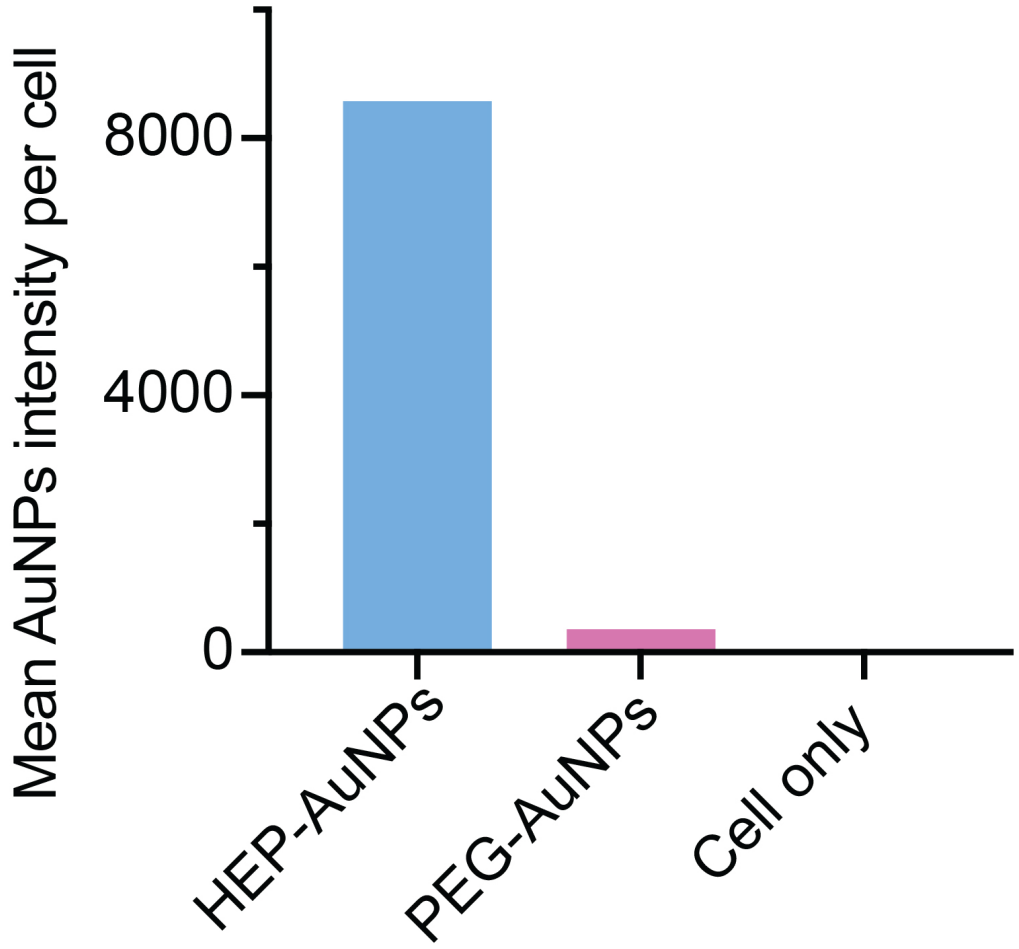

Figure S17. Quantification of the light scattering intensity of nanoparticles in cells.

Light scattering intensities of the gold nanoparticles in Figure 5 were quantified by manually drawing regions of interest around the cell membranes and measuring the integrated density in the light scattering channel on ImageJ.

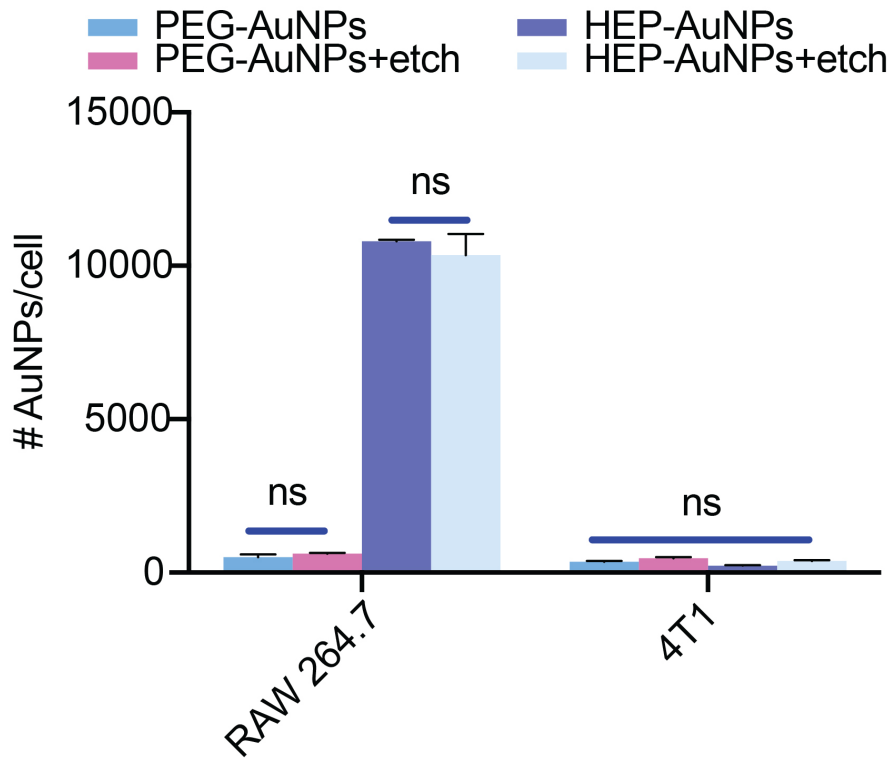

Figure S18. Cell uptake quantification of 15-nm HEP-AuNPs and PEG-AuNPs by ICP/MS in RAW 264.7 macrophages and 4T1 breast cancer cells with and without AuNPs etching.

The 15-nm HEP-AuNPs or control (PEG-AuNPs) were incubated with 4T1 murine breast cancer cells and RAW 264.7 murine macrophages. ICP-MS was performed to quantify the cell uptake of nanoparticles. Around 21x more HEP-AuNPs were internalized than PEG-AuNPs RAW 264.7 macrophage. True nanoparticle internalization was assessed by insensitivity to the KI/I_2 etchant. Bar graphs indicate mean ± SD (n=3-4).

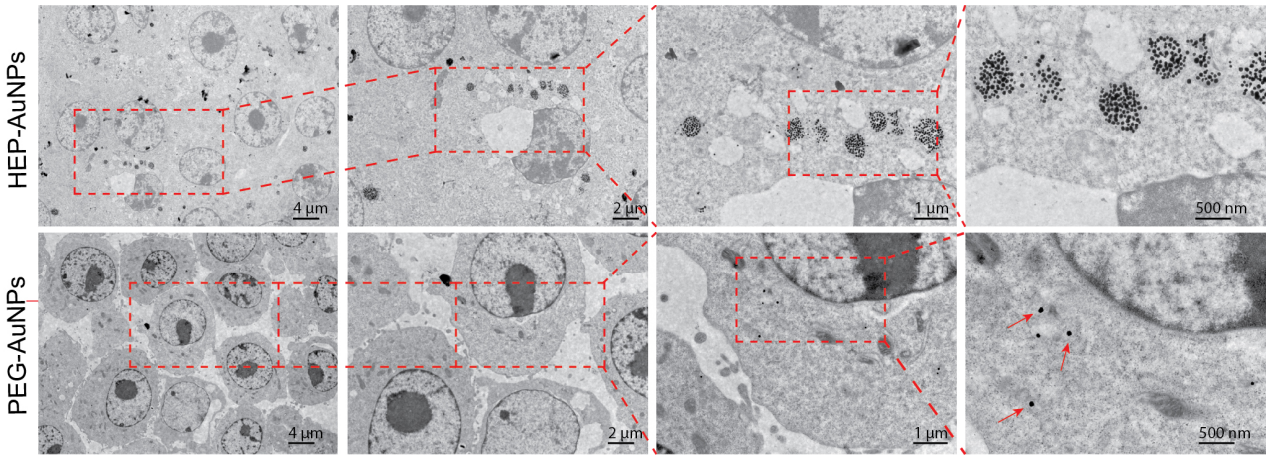

Figure S19. Transmission electron microscopy imaging of the subcellular distribution of 55-nm gold nanoparticles.

After 6 h incubation with 0.3 nM HEP- or PEG-AuNPs, the RAW 264.7 cells were collected and processed for TEM imaging. In TEM, AuNPs are observed as uniform black dots. Note that the magnification increases by ~2-fold in each panel from left to right, and the *dashed red lines* indicate the field of view selected for the next higher magnification. In the case of the less obvious signal with the PEG-coated AuNPs (lower rightmost panel), the *red arrows* indicate several individual AuNPs. The clusters of HEP-AuNPs are much more abundant.

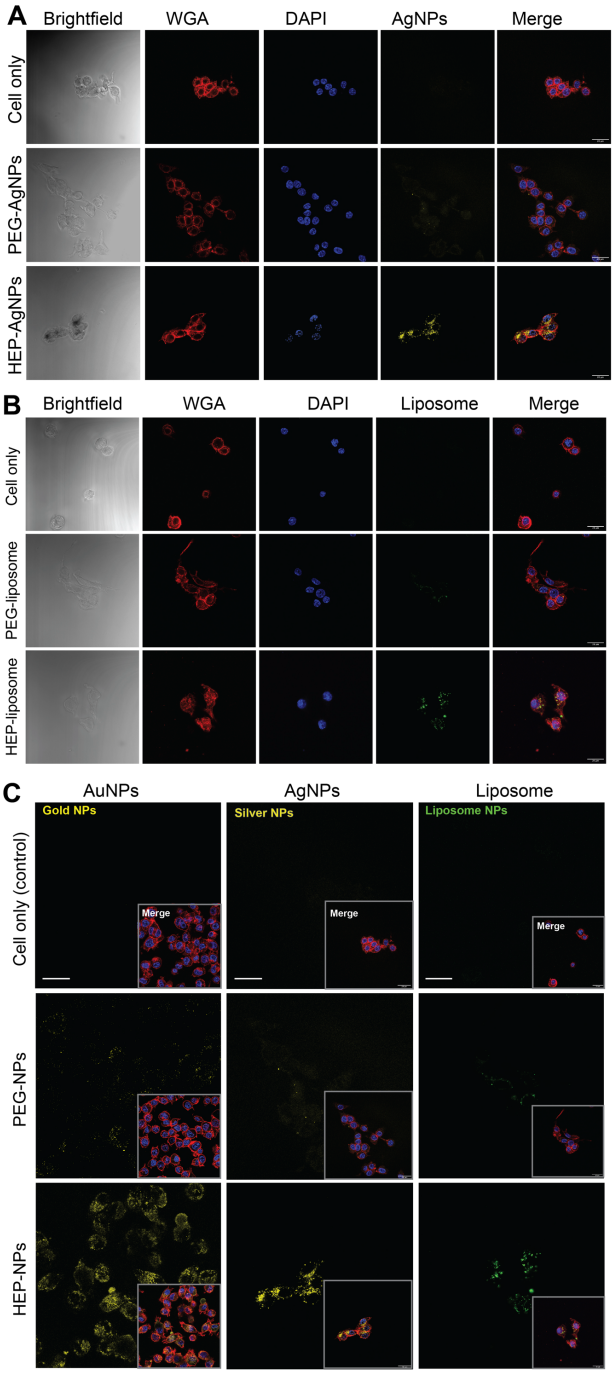

Figure S20. Cellular uptake of silver nanoparticles, liposomes, or gold nanoparticles with various coatings.

(**A-B**) Confocal laser scanning microscopy images (CLSM) of RAW 264.7 cells incubated with either silver nanoparticles (A) or liposome nanoparticles (B) for 2 h and 24 h, respectively. (**C**) CLSM images of HEP-coated gold, silver, and liposome uptake compared with nanoparticles with PEG coating and 'cell only' groups in DC 2.4 dendritic cell (gold nanoparticles) and RAW 264.7 cells (silver nanoparticles and liposomes).

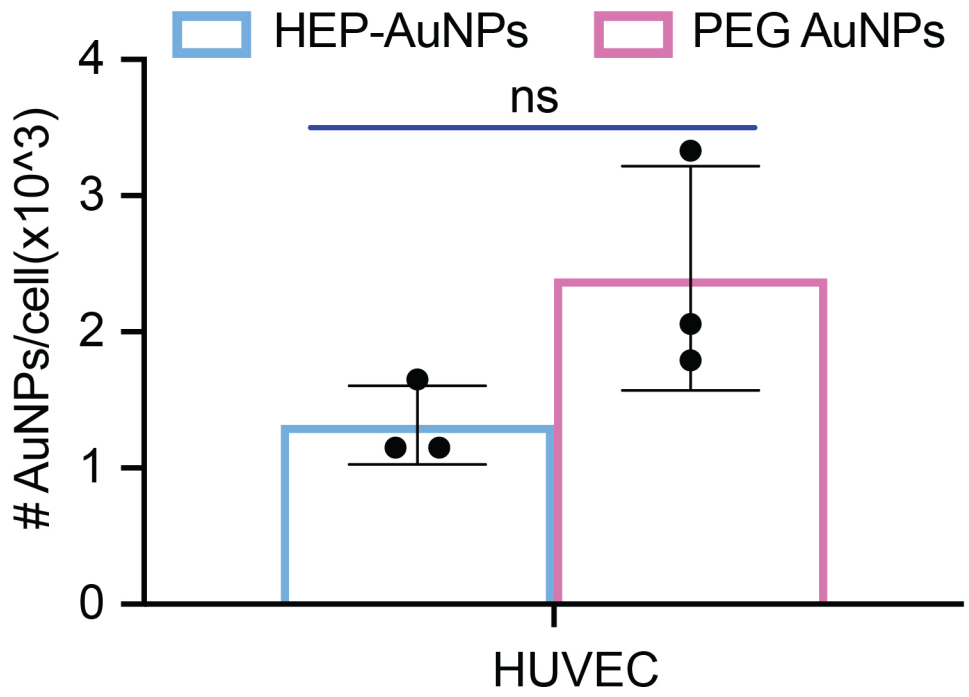

Figure S21. Cell uptake of polymer-coated 55-nm AuNPs in HUVEC endothelial cells.

Human endothelial cells were incubated with HEP-AuNPs or PEG-AuNPs. Nanoparticle cell uptake was quantified by ICP-MS. There was no difference in uptake between the two coated AuNPs. A T-test was used for statistical analysis (mean SD; n=3-4).

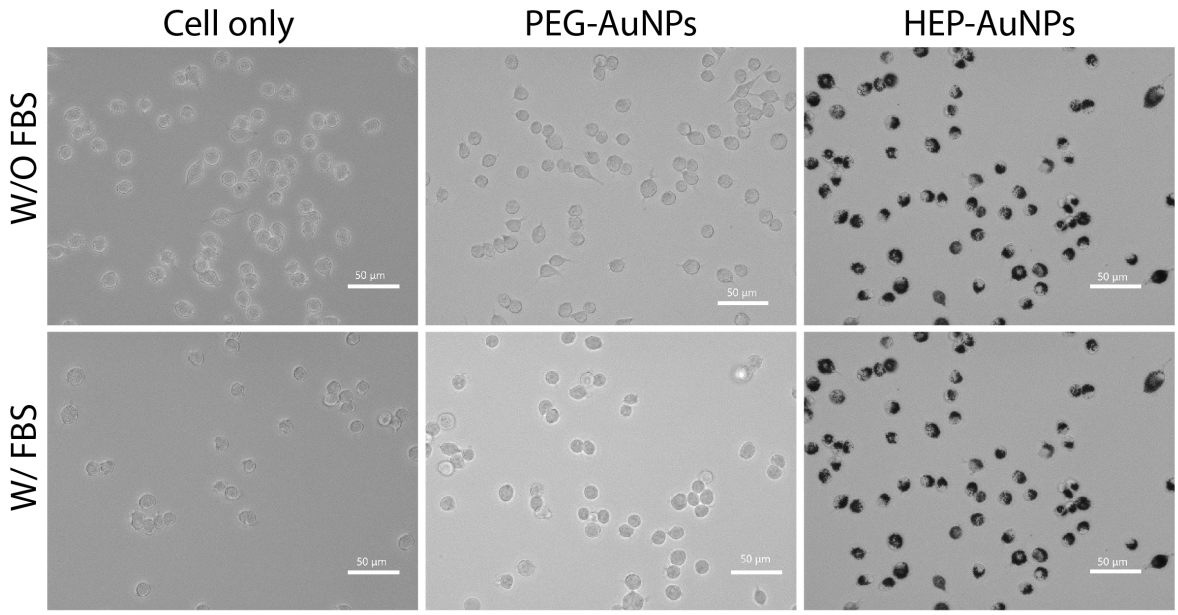

Figure S22. The effect of FBS incubation on cellular uptake.

Either 0.2nM HEP-AuNPs or PEG-AuNPs were incubated with DC 2.4 dendritic cells with or without FBS for 6 hours. Cells were imaged with a brightfield light microscope after removing uninternalized AuNPs. Scale bars represent 50 μm.

Tables

Table S1. Summary of proteins identified from LC/MS-MS.

Abbrev	Full Name	MW[1] (Da)	Biological Process
KNG1	Kininogen-1	71,957	Blood coagulation, Hemostasis, Inflammatory response
HBBF	Hemoglobin fetal subunit beta	15,859	Oxygen transport
IBP2	Insulin-like growth factor-binding protein 2	34,015	Growth regulation
IGF2	Insulin-like growth factor II	19,682	Carbohydrate metabolism, Glucose metabolism, Osteogenesis
HBA	Hemoglobin subunit alpha	15,184	Oxygen transport
HRG	Histidine-rich glycoprotein	44,471	Blood coagulation, Fibrinolysis, Hemostasis
CO4	Complement C4	101,885	Complement pathway, Immunity, Inflammatory response, Innate immunity
BPT2	Spleen trypsin inhibitor I	10,843	Protease inhibitor, Serine protease inhibitor[2]
FA5	Coagulation factor V	248,983	Blood coagulation, Hemostasis
THRB	Prothrombin	70,506	Acute phase, Blood coagulation, Hemostasis
APOC3	Apolipoprotein C-III	10,692	Lipid degradation, Lipid metabolism, Lipid transport
APOE	Apolipoprotein E	35,980	Lipid transport, Transport
ALBU	Albumin	69,293	Cellular response to starvation, negative regulation of apoptotic process
FETUA	Alpha-2-HS-glycoprotein	38,419	Acute-phase response, negative regulation of bone mineralization, positive regulation of phagocytosis
A1AG	Alpha-1-acid glycoprotein	23182	Acute-phase response, regulation of immune system process
TSP4	Thrombospondin-4	105974	Cell adhesion, Tissue remodeling, Unfolded protein response

[1] MW: Molecular weight. [2] Molecular function.

Table S2. LC-MS/MS analysis of surface adsorbed proteins from 55-nm HEP-AuNPs.

	Spectral counts of proteins from HEP-AuNPs at different coating densities (HEP/nm^2)						
Abbrev	0	0.01	0.1	0.25	0.5	1	3
CO4	0.15	0.11	0.45	0.64	0.66	0.66	0.54
KNG1	0.76	0.46	0.10	0.00	0.01	0.03	0.02
HBA	0.28	0.64	0.78	0.45	0.32	0.37	0.36
THRB	1.00	0.42	0.77	0.09	0.03	0.00	0.00
IBP2	0.32	0.79	0.67	0.41	0.03	0.01	0.06
APOE	0.33	0.98	0.21	0.00	0.17	0.05	0.00
FETUA	0.01	0.02	0.40	0.38	0.17	0.02	0.03
HBBF	0.10	0.49	0.64	0.42	0.52	0.36	0.15
BPT2	0.21	0.32	0.69	0.69	0.27	0.48	0.49
IGF2	0.14	0.50	0.62	0.00	0.00	0.00	0.00
HRG	0.43	0.43	0.67	0.00	0.00	0.00	0.00
A1AG	0.00	0.00	0.67	0.17	0.17	0.00	0.50
ALBU	0.00	0.14	0.68	0.34	0.13	0.03	0.24
TSP4	0.00	0.00	0.07	0.30	0.64	0.31	0.81

Total spectral counts are the average of three or four independent replicates.

Table S3. LC-MS/MS analysis of surface adsorbed proteins from 55-nm PEG-AuNPs.

Abbrev	Spectral counts of proteins from PEG-AuNPs at different coating densities (PEG/nm^2)							
	0	0.01	0.1	0.25	0.5	1	3	5
KNG1	0.75	0.59	0.38	0.09	0.12	0.04	0.11	0.03
HBBF	0.57	0.30	0.67	0.04	0.12	0.34	0.10	0.10
IBP2	0.79	0.51	0.53	0.04	0.00	0.02	0.00	0.00
IGF2	1.00	0.52	0.48	0.00	0.00	0.00	0.00	0.00
HBA	0.44	0.33	0.90	0.24	0.07	0.41	0.22	0.45
HRG	0.83	0.33	0.00	0.00	0.00	0.00	0.00	0.00
CO4	0.20	0.15	1.00	0.00	0.04	0.00	0.00	0.00
BPT2	0.06	0.06	0.55	0.26	0.30	0.38	0.41	0.08
FA5	1.00	0.33	0.67	0.00	0.00	0.00	0.00	0.00
THRB	0.80	0.44	0.88	0.00	0.00	0.02	0.02	0.00
APOC3	0.08	0.17	0.50	0.50	0.50	0.67	0.42	0.42
APOE	0.53	0.19	0.77	0.07	0.06	0.33	0.39	0.09
ALBU	0.05	0.00	0.27	0.02	0.03	0.36	0.35	0.44
FETUA	0.13	0.09	0.47	0.09	0.20	0.48	0.22	0.41

Total spectral counts are the average of three or four independent replicates.

Materials and Methods

1. Nanoparticle synthesis (15-nm, 55-nm, or 100-nm AuNPs; 55-nm AgNPs; and uncoated liposomes)

A redox reaction-based bottom-up synthesis approach was used for the synthesis of 15-nm, 55-nm, or 100-nm AuNPs. Aqua Regia was used to clean the reaction flasks before synthesis. Aqua Regia is prepared as a 3:1 ratio of hydrochloric acid (Sigma-Aldrich, ACS reagent, 37%) and nitric acid (Sigma-Aldrich, ACS reagent, 70%).

1.1 Synthesis of 15-nm gold nanoparticle

Based on a protocol published by Turkevich *et al.*, we synthesized 15-nm gold nanoparticles.[1] Briefly, 98.9 mL nanopure water and 1.0 mL of 0.102M sodium citrate tribasic dihydrate (Sigma-Aldrich) were prepared in aqua regia-cleaned 250 mL Erlenmeyer flask. This flask was then placed on a hot plate with settings of 300 °C and ~200 rpm. When the mixture solution in this flask started boiling, 100 µl of 0.25 M aqueous gold (III) chloride trihydrate (Sigma-Aldrich) was added rapidly, and the stirring speed was increased to ~ 400 rpm. Next, a 7 min timer was set. During this 7 min of reaction, the color of the solution changed from purple to cherry red. After 7 min, the flask was placed on ice to quench the reaction and then stored at 4°C. To prevent nanoparticle aggregation, Tween 20 (Sigma-Aldrich, Molecular Biology, Grade) was added with a final concentration of 0.01% (v/v) Tween20. To concentrate and wash, nanoparticles were centrifuged at 15,000 x*g* for 90 minutes using a ThermoFisher Heraeus Multifuge X3R centrifuge. Both DLS and UV-Vis spectrophotometry measurements were performed for nanoparticle quality assessment.

1.2 Synthesis of 55-nm gold nanoparticles

To synthesize larger nanoparticles, a seed-mediated synthesis protocol from Perrault *et al*. was adopted.[2] The 15-nm seed gold nanoparticles were prepared by the previously described protocol; these 'seed' particles were transferred to a new clean flask to synthesize 55-nm AuNPs. The solutions were added and mixed in the following order at room temperature and 400 rpm: 93.7 mL of nanopure water, 0.967 mL of 15-mM aqueous sodium citrate tribasic dihydrate, 0.967 mL of 25-mM aqueous gold (III) chloride trihydrate, 3.35 mL of citrate-stabilized 2.4-nM 15 nm gold nanoparticles (without the addition of Tween 20), and 0.967 mL 25-mM aqueous hydroquinone (Sigma-Aldrich, ReagentPlus, ≥ 99.0%). The solution turned from light pink into dark wine-red right after the addition of hydroquinone. After the overnight reaction, 1 mL, 10% Tween 20 (v/v) was added to this mixture to get a final Tween 20 concentration around 0.1% (v/v). Nanoparticles were centrifuged at 2,000 x*g* for 120 minutes, and then the supernatant was discarded. Pellets were washed with 0.1% (v/v) Tween 20 and 0.01% (w/v) sodium citrate tribasic dihydrate solution for 3 times following centrifugation at 2,000 x*g* for 30 minutes. Nanoparticles were dispersed in 0.1% (v/v) Tween 20 and 0.01% (w/v) sodium citrate tribasic dihydrate solution, and then both concentration and hydrodynamic diameter were measured by UV-Vis spectrophotometry and DLS, respectively. The nanoparticle dispersion was stored at 4 °C until further use.

1.3 Synthesis of 100-nm gold nanoparticles

To synthesize larger nanoparticles, a seed-mediated synthesis protocol from Perrault *et al.* was adopted.[2] The 15-nm gold nanoparticles were prepared by the previously described protocol; these 'seed' nanoparticles were transferred to a new clean flask to synthesize 100-nm AuNPs. Briefly, the solutions were mixed in the following order at room temperature and 400 rpm: 96.7 mL of nanopure

water, 0.997 mL of 15-mM aqueous sodium citrate tribasic dihydrate, 0.997 mL of 25-mM aqueous gold (III) chloride trihydrate, 0.305 mL of citrate-stabilized 2.4-nM 15 nm gold nanoparticles (without the addition of Tween 20), finally, 0.997 mL of 25-mM aqueous hydroquinone was rapidly injected into the mixture. The color of the solution turned from light pink into dark orange-pink after injection of hydroquinone. This mixture was left to react overnight, 1 mL of 10% Tween 20 (v/v) was added to this mixture to get a final Tween 20 concentration of ~ 0.1%. Nanoparticles were spun down at 500 xg for 120 minutes and then washed by 0.1% (v/v) Tween 20 and 0.01% (w/v) sodium citrate tribasic dihydrate solution for 3 times following centrifugation at 500 x*g* for 30 minutes. After purification, the concentration and hydrodynamic diameter were measured by UV-vis spectrophotometry and DLS, respectively. The nanoparticle dispersion was stored at 4 °C until further use.

1.4 Synthesis of 55-nm silver nanoparticles

A modified one-pot method was adopted for the synthesis of 55-nm citrate-capped silver nanoparticles (AgNPs)[3]. Briefly, tannic acid and sodium citrate tribasic dihydrate were added into 100 mL of boiling nanopure water for final concentrations of 5 mM and allowed to stir vigorously for 15 minutes. Then, 0.1 mL of 250 mM silver(I) nitrate was immediately added to the reaction and boiled for 15 minutes.

1.5 Synthesis of uncoated liposomes and PEG-liposomes

Uncoated liposomes and PEG-coated liposomes were prepared based on a published paper[4]. Briefly, uncoated liposomes with a fluorescent tag for imaging were prepared by adding a stock of 0.44 mg/mL DiO'; DiOC18 (3) (3,3'-Dioctadecyloxacarbocyanine Perchlorate) in chloroform to solid 1,2-distearoyl-sn-glycero-3-phosphocholine (DSPC) and cholesterol (final molar ratio of 1:1.3:0.9, respectively). PEG-liposomes were prepared by using 0.44 mg/mL DiO'; DiOC18(3) (3,3'-Dioctadecyloxacarbocyanine Perchlorate) (solvent is chloroform) dissolved 1,2-distearoyl-sn-glycero-3-phosphocholine (DSPC), cholesterol, and phosphatidylethanolamine modified with 2-kDa polyethylene glycol (DSPE-PEG2000) (final molar ratio of 1:1.3:0.9:0.3). After mixing lipids in the desired ratio, the chloroform was evaporated by a rotary evaporator. The lipid films were suspended in 600 µL of 37 ºC warmed 1x phosphate buffered saline using bath sonication (ultrasonic cleaner Branson CPX8800H at 25 ºC) for approximately 20 min. The mixture was then extruded through a 100-nm polycarbonate filter at 60ºC for 21 cycles. The hydrodynamic diameter was measured by DLS.

2. Heparosan synthesis and characterization of OPSS-HEP conjugation

2.1 Heparosan Synthesis

A quasi-monodisperse 13 kDa-heparosan (HEP) polysaccharide (polydispersity *Mw/Mn* 1.038 +/- 0.005) with a reducing end amino group (HEP-NH2) was synthesized by synchronized, stoichiometrically controlled chemoenzymatic reaction using an amine-containing acceptor, UDP-sugar donors, and PmHS enzyme as described previously.[5] This starting material was employed to create two derivatives: (a) a HEP with a thiol-reactive group (HEP-OPSS) at the reducing terminus, and (b) a radioactive version of the same polymer tagged at the non-reducing terminus ([^{3}H]HEP-OPSS). HEP polymers were quantified using the carbazole assay with a glucuronic acid standard.[6]

The thiol-reactive dithiol-pyridyl (OPSS) group was introduced into the reducing end of various HEP-NH_2 polymers using a 31- to 42-fold molar excess of *N*-succinimidyl 3-(2-pyridyldithio)propionate (SPDP) (ThermoFisher) added as 2 or 4 additions in neat DMSO; the reaction was performed with 6-6.7 mg/mL HEP-NH_2 and 30-37% DMSO solvent final in 0.1 M HEPES, pH 7.2, 5 mM EDTA, at room temperature overnight. The HEP-OPSS target was precipitated by the addition of NaCl (0.1 M final) and 4.8 volumes of isopropanol on ice for 2 hours. The resulting pellet was harvested by centrifugation (1,800 x *g*, 30 min), the supernatant was aspirated, and the pellet was dried (3 min under vacuum or air-dried for 2.25 hours) before re-suspension in water at 4°C overnight. The HEP-OPSS was purified from small MW compounds via either strong anion exchange chromatography or by ultrafiltration.

The HEP-OPSS (~100 mg synthesis scale) was applied to a HiTrap Q strong anion exchange column (5 mL bed; GE Healthcare) equilibrated in Buffer A (10 mM NaOAc, pH 5.8) at 2 mL/min and washed with 4 column volumes (cv) of 100% buffer A. A series of linear gradient steps with NaCl

elution (using B buffer = A + 1 M NaCl in steps of 10 cv of 90A:10B, 4 cv of 60A:40B, and then 1 cv of 40A:60B) removed traces of OPSS from the target. The 0.21-0.5 M NaCl fractions containing the HEP-OPSS target were pooled, precipitated with 2.5 volumes of ethanol (similar process to isopropanol employed above), the pellet suspended in water, and stored at -20°C. Alternatively, the HEP-OPSS (~200 mg synthesis scale) target was purified by repeated ultrafiltration (6 cycles with 3 kDa MWCO membrane; Amicon) against water at room temperature to desalt the sample and to remove any residual SPDP. The presence of the OPSS group on the sugar chain was verified by reaction with SAMSA (a fluorescent thiol activated with base per the manufacturer's instructions; ThermoFisher) and then PAGE analysis.7 A fluorescent band at the appropriate MW was detected, thus indicating the successful installation of the OPSS moiety onto the sugar chain as described later.

Radioactive forms of the HEP-OPSS were created by first end-labeling 100-200 μg HEP-NH_2 with 1.1-9 μCi of UDP-[^{3}H]-GlcNAc (PerkinElmer) and PmHS under reactions conditions similar to nonradioactive HEP-NH_2 synthesis;[5] under these conditions only ~1-2% of the HEP chains (~65 monosaccharide units long) are tagged with a single radioactive sugar thus not significantly altering the overall MW of the preparation. The purified material was then reacted with OPSS as above except: (*i*) a 2,000 to 3,555 molar excess of OPSS was used for 3-4 hrs, (*ii*) the final concentration of HEP-NH_2 was 0.2 mg/mL, and (*iii*) the target was precipitated by the addition of NaCl (0.3 M final) and 3 volumes of ethanol at -20°C for 2 hours. The resulting pellet was harvested by centrifugation (18,000 x*g* for 0.5-1 hr), the supernatant was aspirated, and the pellet was then washed in 70% ethanol/0.1 M NaCl and centrifuged again. The pellet was air-dried, resuspended in water, and then purified by repeated ultrafiltration (6 cycles with 3 kDa MWCO; Amicon) against water. The specific activity of

the final [^{3}H]HEP-OPSS product was measured by liquid scintillation counting and determined to be 93-360 mCi/mmol (7-27 nCi/μg).

2.2 Characterization of OPSS-HEP conjugation

Polyacrylamide gel electrophoresis was conducted to ensure the successful conjugation of OPSS to heparosan molecules. In these tests, 13-kDa OPSS-HEP were reacted with a fluorescent probe with either (i) a free thiol (activated SAMSA Fluorescein; Cat# A685; Invitrogen) or (ii) a thiol-reactive group (Fluorescein-5-Maleimide; Cat# 62245; Thermo Scientific) overnight at room temperature. The 13-kDa HEP-NH_2 without OPSS conjugation was used for control. SAMSA was activated by 0.1 M NaOH at room temperature for 15 min, then neutralized with HCl. Samples of the reaction (2 μg of HEP/lane) were compared to control lanes (13-kDa HEP-NH_2 without OPSS modification) with free probes on 6% polyacrylamide gels (1x TBE, 250 V for 15 min). The gel was first imaged for fluorescence (ChemDoc MP imager; BioRad) to observe the probes (indicating if the OPSS was still reactive or the OPS had been lost after processing, etc.) and then was stained with Alcian Blue (cat# A9186; Sigma-Aldrich) to detect the presence of heparosan.

3. Quantification of HEP- and PEG-coatings using DLS for AuNPs and liposomes

3.1 Saturation curve of gold nanoparticles

This protocol was based on a published paper [8]. Briefly, a constant surface area to volume ratio was maintained for every desired PEG (MW 10 kDa, Laysan Bio) surface density (PEG/nm^2); only the surface modification density conditions were varied. The addition ratios of PEG polymer to nanoparticle surface area were 0, 0.1, 0.25, 0.5, 1, 2 PEG/nm^2 for 15-nm AuNPs. Samples were prepared in triplicate by mixing the DI water, PEG solution, and 15-nm citrate-stabilized AuNPs in order. The vials were vortexed a second time and then left to incubate at room temperature for 30 minutes. After the incubation period passed, the PEG was then fully conjugated to the surface of the nanoparticles, which was verified with the Malvern ZetaSizer using dynamic light scattering (DLS). The DLS measured hydrodynamic diameter, which consists of the gold core diameter and the layer of hydration from the surface-bound molecules. Additionally, the success of the effect of the PEG density on the surface charge of the nanoparticles was qualitatively observed through gel electrophoresis, as described below in the gel electrophoresis section. The heparosan saturation curve was obtained by a similar procedure with the use of the salt aging or pH methods as described below.

3.2 Saturation curve of heparosan coated liposomes

Naked liposomes were coated with lipid-modified heparosan polymers using post-insertional modification as in a published paper [5]. Briefly, 13-kDa heparosan-dipalmitate polymers were mixed with uncoated liposomes, then incubated for 90 min at 37 ºC; these conditions result in efficient incorporation of a HEP-coating on the outer leaflet of the bilayer. The saturation curve was obtained

by mixing 9.71 mg/mL heparosan polymer with uncoated liposome at the percentage of molar ratio of HEP polymer to lipids.

4. HEP-AuNPs prepared by the salt aging method

The coating of heparosan by salt aging on 15-nm gold nanoparticles was based on the Hurst/Zhang method [9,10]. This method entails increasing the concentration of sodium chloride (Sigma) to help the heparosan conjugate attach to the gold nanoparticle surface. Briefly, citrate stabilized AuNPs were obtained that had been prepared as described above. A constant surface area to volume ratio was maintained for every desired heparosan surface density (HEP/nm^2); only the surface modification density conditions were varied. The addition ratios of HEP polymer to nanoparticle surface area were 0, 0.25, 0.5, 1, or 2 HEP/nm^2 for 15-nm AuNPs. According to a published protocol, different HEP coating density conditions were performed for 55-nm and 100-nm gold nanoparticles[8]: the range was 0, 0.01, 0.1, 0.5, 1, or 2 HEP/nm^2. Triplicates were performed for each condition. Nanoparticle and heparosan solution were mixed together in DI water and incubated at room temperature for 20 min. NaCl was added in 0.1 M NaCl increments until the final NaCl concentration reached 0.7 M. Each increment was followed by a 20 min incubation at room temperature before the next addition of NaCl. DLS was performed after the final incubation. Agarose gel electrophoresis was performed as described below in the gel electrophoresis section.

5. HEP-AuNPs and HEP-AgNPs prepared by the pH method

The protocol was adapted and modified from a published paper from Liu's lab[10]. In a different process from the salt aging method described above, pH 3.0 Citrate·HCl buffer or pH 3.0 HCl without citrate was used as a solvent for the heparosan and gold nanoparticle mixture instead of using DI water. A constant surface area was maintained for every target heparosan surface density (HEP/nm^2); only the surface modification density conditions were varied. The addition of HEP polymer to nanoparticle surface reactions were 0, 0.25, 0.5, 1, 2 HEP/nm^2 for 15-nm AuNPs. HEP surface coating density of 55-nm AuNPs were 0, 0.1,0.25, 0.5, 1, or 2 HEP/nm^2. The calculated HEP was added and mixed with acid water, then followed by adding nanoparticles. After a brief vortex, NaCl solution was added in 0.3-M NaCl increments until the final NaCl concentration reached 0.6-M. Each increment was followed by a 20 min incubation at room temperature. DLS was measured after final incubation. Agarose gel electrophoresis was performed as described below in the gel electrophoresis section. The optimized pH method shared the same procedure without the addition of citrate to the acid water. The colloidal stability of the low coating density of HEP was maintained over 390 days with the pH method without citrate addition.

The pH method without citrate addition was used for coating HEP on AgNPs. To attach HEP-OPSS or PEG-OPSS to silver nanoparticles, these reagents were first reduced to HEP-SH or PEG-SH by incubation with Tris(2-carboxyethyl)phosphine hydrochloride (TCEP; Sigma-Aldrich) at a molar ratio of 1:50 for 2 h. This reduction step was employed as the OPSS group does not react efficiently with AgNPs in comparison to AuNPs. The hydrodynamic diameter changes were measured by DLS. Based on the maximum saturation curve we obtained from 55-nm AuNPs by DLS, we added over 5 polymers per nm^2 in the silver nanoparticle coating.

6. HEP-AuNPs prepared by the vortex method

For comparison, instead of using salt aging and pH routes, an experiment was done to modify 15-nm nanoparticles with heparosan-OPSS without the salt aging method or pH, similar to the PEGylation method described above. The main objective of this experiment was to showcase the effectiveness of heparosan coating without salt aging by comparison of the amount of heparosan bound to the nanoparticle surface. For this, conditions for heparosan surface coating reactions were chosen to be 0, 0.1, 0.25, 0.5, 0.75, 1, 1.5, or 2 HEP/nm^2. DLS and gel electrophoresis were performed.

7. Quantification of HEP-coatings 15-nm and 55-nm AuNPs using a radiolabeling strategy

Radioactive heparosan and versions of heparosan-OPSS were mixed in a mass ratio of 1 to 4. This heparosan mixture was used to modify 15-nm or 55-nm AuNPs. By using the salt aging method mentioned above, different densities of heparosan mixture as input surface densities (HEP/nm^2) were used to modify 15-nm and 55-nm AuNPs. The input surface HEP densities for 15 nm were 0.2, 0.5, 1.0, 2.0, or 3.0 HEP/nm^2. For 55-nm AuNPs, the input surface coating reactions were 0.1, 0.25, 0.5, 1.0, or 2.0 HEP/nm^2. After the conjugation process, heparosan-modified AuNPs were centrifuged at 4°C for 30 min and centrifuged at either 15,000 x*g* for 15-nm or 2,000 x*g* for 55-nm. To remove free heparosan, the pellet volume after centrifugation was carefully loaded on 25% Percoll (Amersham) and followed by centrifugation at 4°C (1 h at 15,000 x*g* for 15-nm or 2,000 x*g* for 55-nm AuNPs). The radioactivity was measured by liquid scintillation counting on a Packard Tricarb 2300TR.

8. Transmission electron microscopy

8.1 TEM characterization of HEP- and citrate-AuNPs

Samples were loaded and prepared with negative staining by 2% uranyl acetate (Ted Pella, Inc) on a TEM grid (Ted Pella, Inc)[11]. TEM images were taken by a 200-kV field emission JEOL2010F analytical transmission electron microscope with a DE-12 camera. ImageJ (NIH) was used to analyze TEM images[12].

8.2 TEM characterization of AuNPs inside of cells

RAW 264.7 macrophage cells (~1 million) were seeded in each well of a 6-well-plate overnight. Dispersions of 0.3-nM PEG- or HEP-AuNPs were then incubated with the cells for 6 h. Any uninternalized AuNPs were removed by washing the cells thrice with 1x PBS. Cells were scraped and collected by centrifugation (500 x*g*, 5 min, 25ºC) into a 1.5-mL microcentrifuge tube. The supernatant was removed, and the cell pellets were fixed with a freshly made fixative solution containing (2% glutaraldehyde: 4% paraformaldehyde (v/v) in 0.2 M cacodylate buffer) at room temperature for 1 hour. Samples were stored at 4ºC until sectioning and negative staining (3% lead citrate solution, cat. 22410, Electron Microscopy Sciences). The TEM micrographs were taken with a Hitachi H-7600 Transmission Electron Microscope at the Oklahoma Medical Research Foundation (OMRF) imaging core facility in Oklahoma City, OK.

9. Agarose gel electrophoresis

Gels with 0.5% (m/v) agarose (Fisher BioReagents) and 0.5x TBE buffer (Sigma-Aldrich) were used to analyze HEP coating on AuNPs. Nanoparticle samples were concentrated to ensure visibility and (typically 10 µL/lane) then mixed with 150 mg/mL Ficoll (Research Products International) in a 4:1 ratio for loading into wells. Gels were run at 50 V for 40 min. Gel images were taken with an Azure C600 imager using visible light.

10. Quantifying HEP desorption upon exposure of HEP-coated nanoparticles to human plasma

Radioactive heparosan-modified 15-nm or 55-nm AuNPs were incubated with human plasma or 1x PBS for 12 h, 24 h, or 48 h at 37°C. After centrifugation (15,000 x*g*, 15 min for 15-nm AuNPs; 2,000 x*g*, 15 min for 55-nm AuNPs), radioactivity in the supernatants and pellets was measured with the liquid scintillation analyzer (Tri-carb 2300TR). The percentage of radioactivity is calculated using the following equation:

$$\%\ of\ radioactivity = \frac{radio\ counts\ of\ the\ pellets}{radio\ counts\ in\ the\ supernatant + radio\ counts\ in\ the\ pellets}\ x\ 100\%$$

11. Protein corona formation, isolation, and clean up

11.1 Protein corona formation upon nanoparticle incubation in FBS

The protocol followed published papers[13,14]. Briefly, HEP- or PEG-modified gold nanoparticles were incubated with fetal bovine serum (FBS, ThermoFisher) at a ratio of 10 μL per cm^2 of nanoparticle surface area. This incubation was at 37℃ for 24 hours, performed in triplicate. To remove unbound FBS, three rounds of washing were performed by 500 μL of 1x PBS with 5-mM EDTA and 0.05% (v/v) Tween 20 at 18,000 x*g* for 30 min at 4℃. After the final wash, the nanoparticles were then measured by DLS and assessed with agarose gel electrophoresis as described in previous sections. Similarly, we exposed HEP-, PEG-coated AgNPs, or liposomes to FBS, and measured the hydrodynamic diameter change by DLS.

11.2 Protein isolation

Samples with 50 cm^2 nanoparticle surface area were prepared for FBS incubation, followed by the incubation and washing protocol described in the previous paragraph. After the final wash, resuspend the nanoparticle pellets in the residual solution (15 μL). Next, to isolate proteins from nanoparticles, 8 μL of the 4x LDS buffer (Invitrogen) and 4 μL of the 0.5-M dithiothreitol (DTT) solution were added to the vials. The vials were then incubated at 70℃ for 60 minutes to strip the proteins bound to the surface of the nanoparticles. After the 60-minute incubation, the vials were centrifuged at 18,000 x*g* for 15 minutes to remove nanoparticles. Around 30 μL protein supernatant was collected from each tube; 6.5 μL was reserved for SDS-PAGE. The rest of the proteins were processed with clean-up to remove DTT and LDS.

11.3 Protein cleanup

To remove the DTT and LDS in the remaining protein solutions, the trichloroacetic acid (TCA) / acetone method from published literature was used[14]. Proteins were precipitated by the addition of 950 µL 10% w/v TCA(Sigma) in acetone (ThermoFisher) overnight at –80°C. The next day, the precipitated proteins were collected by centrifugation at 18,000 x*g* for 15 min at 4°C, and the supernatant was discarded. The pellets were first dissolved in 500 µL of 0.03% w/v sodium deoxycholate (Sigma) and then incubated on ice for 30 min after adding 100 µl of 72% (w/v) TCA. The supernatant was removed after centrifugation at 18,000 x*g*, 4°C for 15 min. The pellets were dissolved in 1 mL of acetone. The 1 mL solution was split into aliquots of 400 µL for BCA assay and 600 µL for LC-MS/MS and dried in a fume hood. The pellets were stored at -80°C until LC-MS/MS characterization.

12. SDS-PAGE for protein corona characterization

SDS-PAGE gels procedures were based on protocols from Walkey *et al.*[13,14]. We used 4-12 % NuPAGE™ Bis-Tris precast Protein Gels, 1.0 mm, 12-well (ThermoFisher) with as a PageRuler™ Plus Prestained 10-250 kDa Protein Ladder (ThermoFisher) standards in a mini gel tank (ThermoFisher) for SDS-PAGE. The 6.5-µL samples previously saved (section 11) were then mixed with 2.5 µL of the 4x LDS buffer and 1 µL of the 500-mM DTT solution and incubated for 5 minutes at 95°C. Along with 2 µL of the protein ladder, samples were then carefully injected into the wells on the gel, and the gel was run at 200 V for 55 minutes on ice. Once the gel was done, it was carefully separated from the case, and the gel was submerged in the fixing solution (10% (v/v) acetic acid (Fisher Scientific) and 40% (v/v) ethanol (PHARMCO-AAPER)) in a petri dish overnight at room temperature with gentle agitation. The next morning, the gel was rinsed with DI water and then stained by1x SYPRO™ Tangerine Protein Gel Stain according to the manufacturer's protocol for 60 minutes at room temperature with gentle agitation (wrapped in aluminum foil to avoid light). Stained gel was rinsed with DI water and imaged under Azure C600 with an excitation/emission set compatible with the stain and ladder. ImageJ (NIH) was used to analyze the intensity of each lane on the same SDS PAGE images[13].

13. Liquid Chromatography Tandem Mass Spectrometry (LC-MS/MS)

All chemicals were purchased from Sigma-Aldrich (Milwaukee, WI) unless noted otherwise. Trypsin (TPCK treated) was obtained from ThermoFisher (Rockford, IL).

13.1 Liquid Chromatography Tandem Mass Spectrometry (LC-MS/MS)

The protein pellet was solubilized in 15 µL of 25-mM ammonium bicarbonate. Six M urea, 200-mM dithiothreitol, and 200-mM iodoacetamide were prepared in 25-mM ammonium bicarbonate. The protein solution was incubated with 1 µL of 6-M urea and 1 µL of 200-mM dithiothreitol for 1 h at 37°C for denaturation and reduction. Then the reduced proteins were incubated with 5 µL of 200-mM iodoacetamide for 30 minutes in the dark at room temperature for alkylation. After incubation, 5 µL of 200-mM dithiothreitol was added to the solutions followed by incubation with 3 µL of 0.1-µg/µL trypsin (prepared in 25-mM ammonium bicarbonate) at 37°C and pH 7 overnight. For both the HEP coating and PEG coating, protein digest samples containing varying coating densities were prepared in triplicate. All samples were stored at -20 °C until analysis.

A 15-µL aliquot of the protein digest was injected onto a custom-packed C18 reverse-phase liquid chromatography (RPLC) column (75 µm i.d., 150 mm length, 2 µm C18 resin) for peptide separation. Mobile phase A was 0.1% formic acid in HPLC grade water and mobile phase B was 0.1% formic acid in acetonitrile. The flow was split to result in a flow rate of approximately 0.8 µL/min through the RPLC column. The LC gradient started with sample loading at 0% mobile phase B for 30 min, followed by an increase from 0% to 35% mobile phase B over 120 min. The mobile phase B gradient was increased to 90% over 3 min and was held constant for 5 min. Mobile phase B was then decreased

to 0% over 2 min and maintained for 50 min for column re-equilibration. The eluted peptides were analyzed using an LTQ mass spectrometer (Thermo Fisher Scientific, Hanover Park, IL, USA) with a custom nano-ESI interface[15]. The heated capillary temperature was 275°C with a spray voltage of 3.5 kV. MS scans were obtained with a normal scan rate and the m/z range was 350-1350. MS/MS scans were acquired using ITMS with collisional induced dissociation (CID) at a normalized collision energy setting of 35%. The ten most abundant precursor ions were selected for MS/MS. The AGC for MS/MS was 3E4 and the maximum ion injection time was 50 ms with 3 microscans. The column was washed between sample runs by injecting a buffer blank and running the same gradient setup.

13.2 Analysis of LC-MS/MS Spectra and cluster

Peptides were identified using MSGF+ to search the mass spectra from the LC-MS/MS analysis against the annotated bovine database downloaded from www.uniprot.org (proteome ID is UP000009136)[16]. A decoy database was automatically generated by MSGF+. Peptide identifications were filtered using a SpecE value cut-off of 1E-10 (i.e., the calculated FDR < 1% at the unique peptide level).

The database search identified 14 proteins for the HEP coating and 14 proteins for the PEG coating, excluding proteins identified in only a single experimental replicate. Identified proteins with relative abundance (by mass) less than 0.25% in one coating density were also excluded [14,17]. The spectral count of the same identified protein in each experimental set was normalized using the highest value. The average normalized spectral counts for the identified protein in triplicate sets are reported in Table S2 and Table S3 for the HEP and PEG coatings. The identified proteins for the HEP and PEG coatings were clustered using the "clustergram" function in MATLAB. Pearson correlation

coefficient and unweighted average distance were used as a distance metric. The relative abundance of proteins in the same cluster were summed and plotted as a function of the coating densities[14].

14. BCA-based protein quantification assays

The commercial BCA (bicinchoninic acid) assay was used to quantify the protein concentration (cat. 23225, ThermoFisher). The purified protein pellets were dissolved in 40 µL of 2% (w/v) SDS dispersed in 1XPBS. 50-µL aliquots of serially diluted concentration of bovine serum albumin (BSA, Pierce) or 10 µL of each sample were placed into 96 well plates. Next, 200 µL of freshly made BCA working solution was added to each well, then incubated at 37ºC for 1 hour. Absorbance at 562 nm was measured by a plate reader (BioTek Synergy Neo2 Multi-Mode Plate Reader). The protein concentrations were calculated based on the BSA standard protein curve.

15. Cell viability tests

Cell viability assay was performed as previously described[18]. Briefly, cells were grown in 96-well plates at a density of 3.5×10^3 cells/well overnight in the presence of recommended complete media containing 10% (v/v) fetal bovine serum (cat. 16000-044, Life Technologies) and 1% (v/v) pen-strep (cat. 15140-122, Life Technologies). After overnight incubation, media was aspirated, and cells were then treated with either various doses of gold nanoparticles or PBS at a final volume of 100 μL per well. After 48 h incubation, cells were washed with PBS thrice, and the cell viability was determined using the XTT assay (2,3-Bis-(2-Methoxy-4-Nitro-5-Sulfophenyl)-2H-Tetrazolium-5-Carboxanilide, cat. 11465015001, Sigma) according to the manufacturer's protocol. The cell viability as a readout of absorbance of formazan in dimethyl sulfoxide (DMSO) at 570 nm was expressed as a percentage (%) of cells that remained live.

16. Hemolysis assays

The hemolysis assay procedures were adopted from published papers[19,20]. Briefly, 100 µL of 10% of washed human red blood cells (2% packed cells final; Innovative research) were incubated with PEG- or HEP-coated AuNPs (1 nM final in 400 µL volume of 1x PBS) at 37ºC for 3 h. Triton-X 100 and 1x PBS were used for the positive and negative controls, respectively. Blood-free samples (without incubation of human red blood cells) were also prepared to account for the intrinsic absorbance of AuNPs. After the incubation, all samples were centrifuged at 10,050 x*g* for 30 min at room temperature. A 100-µL aliquot of the supernatant was transferred into a 96 well plate, and the absorbance of hemoglobin at a wavelength of 577 nm was measured. The values of the blood-free samples were lower than the negative control, thus no interference from the AuNPs was observed. The hemolysis percentage was calculated according to the following equation:

$$\%\ hemolysis = \frac{(absorbance\ of\ sample - absorbance\ of\ blank)}{(absorbance\ of\ positive\ control - absorbance\ of\ blank)}\ \text{x}100\%$$

17. Cytokine release assay

As a measure of biocompatibility, the levels of various proteins known to be involved in stress and inflammatory reactions were analyzed after treatment with various nanoparticles. RAW 264.7 macrophages were seeded in 48-well-plates overnight (2E5 cells per well). Then either 1x PBS (control) or suspensions of 0.06-nM of 55-nm citrate-, PEG-, or HEP-AuNPs were added to cells for 24 h. The supernatants were collected and washed by centrifuging at 15,000 x*g* for 15 min twice. Aliquots of the supernatants were incubated with Mouse Cytokine Array Panel A Detection Antibody Cocktail (Proteome Profiler Mouse Cytokine Array Kit, Panel A, ARY006, R & D Systems, Minneapolis, MN 55413) for 1 h. The sample/antibody mixtures were then incubated with the array membranes overnight at 4°C. After washing, the membranes were incubated with HRP-conjugated secondary antibody for 30 min. For blotting development, 1 mL of Chemi Reagent Mix was applied to each of the membranes, followed by chemiluminescence film (BX810, Midsci, St. Louis, MO 63088) exposure for 24 h to get the optimal images. Blot images were quantified by the Quick Spot image analysis tool.

18. Nanoparticle cell uptake studies

The cell uptake protocols follow previously published precedures[8]. Briefly, human endothelial cells (HUVECs), J774A.1, and RAW 264.7 macrophages were purchased from ATCC, USA. First, a total of $3x10^5$ cells/well were seeded onto a 24-well plate and allowed to adhere overnight. The cells were washed with sterile 1x phosphate buffered saline (PBS) thrice, then 1 mL of nanoparticles (0.3 nM final) in the corresponding cell media with FBS were administered and incubated for 6 h at 37°C (5% CO_2) in a humidified tissue culture incubator.

To assess the effect of FBS on cellular uptake studies, after seeding overnight, the cells were 'cleansed' by incubating in cell media without FBS for 30 min at 37°C. Then the cells were washed with sterile 1x phosphate buffered saline (PBS) thrice, and 1 mL of 0.2-nM nanoparticles in either complete cell media or FBS-free cell media were added to cleansed cells for 6 h incubation at 37°C (5% CO_2) as above.

After incubation with nanoparticles, cells were washed with 2 mL of 1 X PBS thrice to remove non-internalized nanoparticles. Purified cell samples were then digested by adding 500 µL of Aqua Regia (1-part nitric acid, 3-part hydrochloric acid, v/v) directly into the wells. After 30 min, the acid-digested samples were transferred to 1.5-mL microcentrifuge tubes and placed in a water bath at 70°C for 1 h to complete the digestion process. Samples were then allowed to cool and then diluted 40-fold into nanopure water with a final volume of 5 mL. All elemental analysis measurements for nanoparticle uptake were done using the PerkinElmer NexIon 2000 ICP-MS on the Prepfast IC Sample Introduction system at the Mass Spectrometry Facility, University of Oklahoma. To

determine the average number of nanoparticles per cell, the dissolved gold signal was correlated to the magnesium signal from known cell numbers. Cell samples were then analyzed for both gold and magnesium signals. Iridium was used as an internal standard. Data was analyzed on GraphPad Prism.

19. Confocal laser scanning microscopy studies

DC 2.4 dendritic cells were seeded onto sterile glass coverslips placed into a 6 well-plate overnight with RPMI 1640 culture media supplemented with 10% fetal bovine serum and 1% Penicillin-Streptomycin. The next day cell media was removed. 0.2 nM PEG- or HEP-coated 55-nm gold nanoparticles were administrated for a 3 h incubation. Cells were washed thrice with PBS to remove noninternalized gold nanoparticles. Cells were fixed by 4% paraformaldehyde (PFA, cat# AAJ19943K2, Thermo Fisher) at room temperature for 10 minutes. Fixed cells were stained with wheat germ agglutinin CF633 (WGA, cat# 29024, Biotium) and NucBlue DAPI (cat# R37606, Thermo Fisher) according to the manufacturer's protocols to label the cell surface or the nuclei, respectively. Confocal images were taken with a 63x oil immersion objective (1.4 NA) on a ZEISS LSM 880 inverted confocal laser scanning microscope (CLSM) using photomultiplier tube (PMT) detectors with a 405-nm diode laser and a 633-nm helium-neon laser for fluorescent channels through a main beam splitter (MBS) 488/561/633 filter. The nanoparticles were imaged using light scattering principles described by Jiang *et al.*[21,22] with a 561-nm diode-pumped solid-state laser and an MBS T80/R20 filter. Light scattering intensities of the gold nanoparticles were quantified by manually drawing regions of interest around the cell membranes and measuring the integrated density in the light scattering channel on ImageJ. Typical measurements were the result of imaging 25 cells/condition.

Similarly, we studied the cellular uptake of HEP- or PEG-coated AgNPs and liposomes in RAW 264.7 macrophages. Silver and liposome nanoparticles were incubated with cells seeded in 96 well-plates. After fixing and staining, cells were scraped down and dropped on glass slides, then covered

by another glass slips to image silver and liposome samples. The same confocal setup was used for AgNPs. Liposomes labeled with DiO'; DiOC18(3) (3,3'-Dioctadecyloxacarbocyanine Perchlorate) (DIO, cat# D275, ThermoFisher) were imaged using a 488-nm laser for the fluorescent channel, but the rest of the procedures were the same.

20. UV-Vis spectrophotometry-based depletion assay

We adopted a previously published protocol to obtain a maximum loading capacity of 10-kDa PEG-OPSS on 15-nm gold nanoparticles[8]. Briefly, PEGylated gold nanoparticles were centrifuged at 15,000 X *g* for 30 min. The supernatant was separated from gold nanoparticle pellets and measured at 283 nm by a UV-Vis-NIR spectrophotometer (Agilent Cary 5000). The absorbance differences between the added PEG and the supernatant were the absorbance of PEG conjugated to gold nanoparticles. We defined the absorbance of PEG conjugated to gold nanoparticles as ΔAb. The point at which ΔAb does not increase is defined as the saturation point.

Supplementary References

(1) Turkevich, J.; Stevenson, P. C.; Hillier, J. A Study of the Nucleation and Growth Processes in the Synthesis of Colloidal Gold. *Discuss. Faraday Soc.* **1951**, *11* (0), 55–75. https://doi.org/10.1039/DF9511100055.

(2) Perrault, S. D.; Chan, W. C. W. Synthesis and Surface Modification of Highly Monodispersed, Spherical Gold Nanoparticles of 50−200 Nm. *J. Am. Chem. Soc.* **2009**, *131* (47), 17042–17043. https://doi.org/10.1021/ja907069u.

(3) Bastús, N. G.; Merkoçi, F.; Piella, J.; Puntes, V. Synthesis of Highly Monodisperse Citrate-Stabilized Silver Nanoparticles of up to 200 Nm: Kinetic Control and Catalytic Properties. *Chem. Mater.* **2014**, *26* (9), 2836–2846. https://doi.org/10.1021/cm500316k.

(4) Syed, A. M.; MacMillan, P.; Ngai, J.; Wilhelm, S.; Sindhwani, S.; Kingston, B. R.; Wu, J. L. Y.; Llano-Suárez, P.; Lin, Z. P.; Ouyang, B.; Kahiel, Z.; Gadde, S.; Chan, W. C. W. Liposome Imaging in Optically Cleared Tissues. *Nano Lett.* **2020**, *20* (2), 1362–1369. https://doi.org/10.1021/acs.nanolett.9b04853.

(5) Lane, R. S.; Haller, F. M.; Chavaroche, A. A. E.; Almond, A.; DeAngelis, P. L. Heparosan-Coated Liposomes for Drug Delivery. *Glycobiology* **2017**, *27* (11), 1062–1074. https://doi.org/10.1093/glycob/cwx070.

(6) Bitter, T.; Muir, H. M. A Modified Uronic Acid Carbazole Reaction. *Analytical Biochemistry* **1962**, *4* (4), 330–334. https://doi.org/10.1016/0003-2697(62)90095-7.

(7) Sismey-Ragatz, A. E.; Green, D. E.; Otto, N. J.; Rejzek, M.; Field, R. A.; DeAngelis, P. L. Chemoenzymatic Synthesis with Distinct Pasteurella Heparosan Synthases: Monodisperse Polymers and Unnatural Structures. *J. Biol. Chem.* **2007**, *282* (39), 28321–28327. https://doi.org/10.1074/jbc.M701599200.

(8) Lee, J. C.; Donahue, N. D.; Mao, A. S.; Karim, A.; Komarneni, M.; Thomas, E. E.; Francek, E. R.; Yang, W.; Wilhelm, S. Exploring Maleimide-Based Nanoparticle Surface Engineering to Control Cellular Interactions. *ACS Appl. Nano Mater.* **2020**, *3* (3), 2421–2429. https://doi.org/10.1021/acsanm.9b02541.

(9) Hurst, S. J.; Lytton-Jean, A. K. R.; Mirkin, C. A. Maximizing DNA Loading on a Range of Gold Nanoparticle Sizes. *Anal. Chem.* **2006**, *78* (24), 8313–8318. https://doi.org/10.1021/ac0613582.

(10) Zhang, X.; Servos, M. R.; Liu, J. Instantaneous and Quantitative Functionalization of Gold Nanoparticles with Thiolated DNA Using a PH-Assisted and Surfactant-Free Route. *J. Am. Chem. Soc.* **2012**, *134* (17), 7266–7269. https://doi.org/10.1021/ja3014055.

(11) Liu, L. Y.; Ma, X.-Z.; Ouyang, B.; Ings, D. P.; Marwah, S.; Liu, J.; Chen, A. Y.; Gupta, R.; Manuel, J.; Chen, X.-C.; Gage, B. K.; Cirlan, I.; Khuu, N.; Chung, S.; Camat, D.; Cheng, M.; Sekhon, M.; Zagorovsky, K.; Abdou Mohamed, M. A.; Thoeni, C.; Atif, J.; Echeverri, J.; Kollmann, D.; Fischer, S.; Bader, G. D.; Chan, W. C. W.; Michalak, T. I.; McGilvray, I. D.; MacParland, S. A. Nanoparticle Uptake in a Spontaneous and Immunocompetent Woodchuck Liver Cancer Model. *ACS Nano* **2020**, *14* (4), 4698–4715. https://doi.org/10.1021/acsnano.0c00468.

(12) Schneider, C. A.; Rasband, W. S.; Eliceiri, K. W. NIH Image to ImageJ: 25 Years of Image Analysis. *Nat. Methods* **2012**, *9* (7), 671–675. https://doi.org/10.1038/nmeth.2089.

(13) Walkey, C. D.; Olsen, J. B.; Song, F.; Liu, R.; Guo, H.; Olsen, D. W. H.; Cohen, Y.; Emili, A.; Chan, W. C. W. Protein Corona Fingerprinting Predicts the Cellular Interaction of Gold and Silver Nanoparticles. *ACS Nano* **2014**, *8* (3), 2439–2455. https://doi.org/10.1021/nn406018q.

(14) Walkey, C. D.; Olsen, J. B.; Guo, H.; Emili, A.; Chan, W. C. W. Nanoparticle Size and Surface Chemistry Determine Serum Protein Adsorption and Macrophage Uptake. *Journal of the American Chemical Society* **2012**, *134* (4), 2139–2147. https://doi.org/10.1021/ja2084338.
(15) Fang, M.; Wang, Z.; Cupp-Sutton, K. A.; Welborn, T.; Smith, K.; Wu, S. High-Throughput Hydrogen Deuterium Exchange Mass Spectrometry (HDX-MS) Coupled with Subzero-Temperature Ultrahigh Pressure Liquid Chromatography (UPLC) Separation for Complex Sample Analysis. *Analytica Chimica Acta* **2021**, *1143*, 65–72. https://doi.org/10.1016/j.aca.2020.11.022.
(16) Kim, S.; Pevzner, P. A. MS-GF+ Makes Progress towards a Universal Database Search Tool for Proteomics. *Nature Communications* **2014**, *5* (1), 5277. https://doi.org/10.1038/ncomms6277.
(17) Griffin, N. M.; Yu, J.; Long, F.; Oh, P.; Shore, S.; Li, Y.; Koziol, J. A.; Schnitzer, J. E. Label-Free, Normalized Quantification of Complex Mass Spectrometry Data for Proteomic Analysis. *Nat Biotechnol* **2010**, *28* (1), 83–89. https://doi.org/10.1038/nbt.1592.
(18) Hossen, Md. N.; Rao, G.; Dey, A.; Robertson, J. D.; Bhattacharya, R.; Mukherjee, P. Gold Nanoparticle Transforms Activated Cancer-Associated Fibroblasts to Quiescence. *ACS Appl. Mater. Interfaces* **2019**, *11* (29), 26060–26068. https://doi.org/10.1021/acsami.9b03313.
(19) Huang, H.; Lai, W.; Cui, M.; Liang, L.; Lin, Y.; Fang, Q.; Liu, Y.; Xie, L. An Evaluation of Blood Compatibility of Silver Nanoparticles. *Scientific Reports* **2016**, *6* (1), 25518. https://doi.org/10.1038/srep25518.
(20) Dobrovolskaia, M. A.; Clogston, J. D.; Neun, B. W.; Hall, J. B.; Patri, A. K.; McNeil, S. E. Method for Analysis of Nanoparticle Hemolytic Properties in Vitro. *Nano Lett.* **2008**, *8* (8), 2180–2187. https://doi.org/10.1021/nl0805615.
(21) Wang, F.; Chen, B.; Yan, B.; Yin, Y.; Hu, L.; Liang, Y.; Song, M.; Jiang, G. Scattered Light Imaging Enables Real-Time Monitoring of Label-Free Nanoparticles and Fluorescent Biomolecules in Live Cells. *J. Am. Chem. Soc.* **2019**, *141* (36), 14043–14047. https://doi.org/10.1021/jacs.9b05894.
(22) Syed, A. M.; Sindhwani, S.; Wilhelm, S.; Kingston, B. R.; Lee, D. S. W.; Gommerman, J. L.; Chan, W. C. W. Three-Dimensional Imaging of Transparent Tissues via Metal Nanoparticle Labeling. *J. Am. Chem. Soc.* **2017**, *139* (29), 9961–9971. https://doi.org/10.1021/jacs.7b04022.